Direction de la recherche technologique
Département des Technologies Hydrogène - DTH
Laboratoire des Technologies de l'Hydrogène - LTH

Rapport technique DTH/DR/2006/14

DEPOT DE ZrC POUR LES REACTEURS HAUTE TEMPERATURE

C. DESRATS - O. DUGNE - A. MERLAU - M. PEREZ- L. OBRINGER

Référence du contrat	A CDHTR (HTR-F1)
Référence PRODEM	01-00143-A
Nature du rapport	Final
Confidentialité	Les informations contenues dans ce document sont régies par les clauses de confidentialité de l'accord Tripartite, elles sont à l'usage des seuls destinataires désignés et ne doivent en aucun cas être transmises à des personnes ou organismes extérieurs à cet accord.

	Rédacteur	**Vérificateur**	**Approbateur**
Nom	Marc PEREZ	Emmanuel RIGAL	Philippe BUCCI
Fonction	Chef de projet	Ingénieur	Chef de laboratoire
Signature			
Date	16/02/2006	27.02.06	27.02.2006

LISTE DE DIFFUSION

Rapport complet à:

CLIENT	**FRAMATOME ANP**	
	D. HITNER	5 ex.
	M. PASQUET	1 ex.
	P. GUILLERMIER	1 ex.
	F. CELLIER	1 ex.
	EDF/R&D	
	F. VASSEUR	5 ex.
SAC/DEN/DDIN/SF	F. CARRE	1 ex.
	Ph. BROSSARD	1 ex.
	C. RENAUD	1 ex.
CAD/DEN/DER/SESI	D. BARBIER	1 ex.
CAD/DEN/DEC/SESC	M. PHELIP	1 ex.
CAD/DEN/DEC/SPUA/LCU	F. CHAROLLAIS	1 ex.
LITEN	D. MARSACQ	1 ex.
	B. VINET	1 ex.
DTH/Dir	H. BURLET	1 ex.
LABORATOIRE	Ph. BUCCI	1 ex.
	Auteur (s)	1 ex.
	Archivage	Original + 1 ex.
BASE HTREX	htrex@cea.fr	1 ex. format PDF

Page de garde + résumé + Liste de diffusion à :

Chef de département DEN/CAD/DEC

Chefs des autres Laboratoires du DTH :

- LEV : LEFEBRE-JOUD Florence
- LPAC : ANTONI Laurent
- UTIAC : DE DINECHIN Guillaume

Page de garde + résumé + Liste de diffusion + Lettre d'envoi à :

Ingénieur Qualité : JF. NOWAK

Bureau financier (Ventes) : S. VERMET

EUROPEAN COMMISSION

5th EURATOM FRAMEWORK PROGRAMME
KEY ACTION: NUCLEAR FISSION

HTR -F1

High-Temperature Reactor Fuel Technology

CONTRACT N°
FIKI-CT-2001-00150

ZrC innovative coating

M. PEREZ

C. DESRATS - O. DUGNE – A. MERLAU - L. OBRINGER, Technical Support

Commissariat à l'Energie Atomique - FRANCE

Dissemination level: RE

Document Number: HTR-F1-05/11-D-4.3.1

First Version

Deliverable Number: 4.3

Abstract

In order to use a particle fuel in very high temperature conditions, the silicon carbide layer which provides a barrier between metal fission products needs to be replaced by zirconium carbide. This material is considered one of the most promising and has been put forward for the VHTR (Very High Temperature Reactor, Génération-IV). Chemical vapour deposition (or CVD) in a fluidised bed is used as the coating technique.

In the literature review, ZrC properties are compared to those of the SiC, the various processes using its precursors are listed and this list is then integrated within a thermodynamic study in order to find the ideal mix for a stoichometric cotaing of ZrC.

This mixture will contain the gaseous precursors $ZrCl_4$, C_3H_6 or CH_4, Ar and H_2. A Specific apparatus has been added to the deposition furnace for zirconium chlorination. It was used to carry out a series of experiments on yttrium stabilised zirconia kernels to simulate the fuel. Specific characterisations were carried out on the deposited material.

Keywords

Very high temperature reactor (VHTR), zirconium carbide (ZrC), chemical vapour deposition (CVD), fluidised bed coating, ZrC coating, coating, nuclear "fuel", chlorination.

Table of contents

INTRODUCTION

This work was carried out as part of a collaborative project at a Europe-wide level, aiming to develop fuel kernel coating techniques. The process, also known as TRISO coating, is carried out by means of a Chemical Vapour Deposition (CVD) technique in a fluidised bed. Fuel coating is a vital aspect for the thermal neutron coolant system (HTR, VHTR, etc.). After having surveyed past discoveries in the area, we attempted to increase the particles' heat resistance and to determine the properties of the various layers of fuel coating in order to model its behaviour and the effects of irradiation. The aim was to obtain experimental particles with improved characteristics in terms of mechanical strength and corrosion resistance in order to give such particles enhanced reliability. It was therefore necessary to develop materials that are more inert than silicon carbide (SiC), which can tolerate contact with fuel or its fission products. Studies carried out in Japan on replacing SiC by zirconium carbide (ZrC) have demonstrated that integrity can be guaranteed up to 2,000°C.

I Comparison of SiC and ZrC properties

This part of the study focuses on the properties of zirconium carbide and compares them with those of silicon carbide to ensure that ZrC meets the required conditions and can provide a useful substitute for SiC in the domain of nuclear fuel particles.

1.1 Thermal properties

1.1.1 Fusion temperature

ZrC has a much higher fusion temperature than SiC. For Zr-C, the phase diagram gives T_{fmax}=3,427±20°C for 43.8 % at. C and Tf ≅ 2,876°C for perfectly stoichometric ZrC. By comparison, for SiC, T_{fmax} = 2,545±40 °C [1].

The following advantages could be gained:

- during manufacturing of the moderator/particle fuel rods, the graphite matrix containing particles is then treated both to remove gas from the element and to increase its density. This treatment could take place at a higher temperature than 1,900°C, the current temperature limit for SiC compounds. A graphite matrix with better crystallisation could thus be obtained, with, in particular, an improvement in its thermal conductivity and radiation resistance [2]
- the reactor could give a better yield by having a higher coolant temperature at core output. The Japanese studies demonstrated that the particles remain intact up to approximately 2,400°C for operation at 1.5 % FIMA (∗) and up to 1,730°C at 4.5 % FIMA, with degradation beyond this level, maybe perhaps due to thermal expansion of the kernels [3][4].

(∗) Number of fissions per initial metal atom ; a measurement of metallurgical damage in the fuel as a whole, i.e. fissile and fertile atoms.

1.1.2 Thermal conductivity

Under normal pressure and temperature conditions, thermal conductivity (λ) for SiC is 25.5 $W.m^{-1}.°C^{-1}$ and for ZrC is 20.5 $W.m^{-1}.°C^{-1}$. However, for high temperatures, $\lambda_{ZrC,1,600K}$ = 23 $W.m^{-1}.°C^{-1}$ and $\lambda_{ZrC,2.000K}$ = 23.5 $W.m^{-1}.°C^{-1}$ whereas $\lambda_{SiC,1.600K}$ = 11 $W.m^{-1}.°C^{-1}$ [5]. The thermal conductivity of ZrC is thus twice as a high as that of SiC at high temperature.

1.2 Mechanical and chemical properties

1.2.1 Corrosion resistance

ZrC has a good compatibility with the fuel kernel and fission products. Japanese studies have confirmed that ZrC shows no sign of corrosion by palladium produced by fission, as is seen with SiC at high temperatures by accumulation of Pd at the interface. The most likely explanation is that Pd diffusing through the layer does not reach a high enough concentration to corrode ZrC. Studies are currently underway to confirm this result. The solution would be to add a further layer to trap Pd, for instance a SiC-C composite before or after the ZrC layer [4], [6].
Japanese thermodynamic studies have shown that, in the event of an accident, ZrC would be subject to passive oxidation.

1.2.2 Mechanical resistance to irradiation

In general, three causes of rupture are cited for HTR particles:
- composite rupture caused by PyC rupture,
- rupture caused by internal pressure from fission gas products,
- rupture caused by the amoeba effect (kernel migration).

At LASL (Los Alamos Scientific Laboratories), ZrC samples were subjected to maximum fluence of $10.7*10^{21}$ neutrons.cm^{-2} (neutrons of energy E>0.18 MeV) at a maximum temperature of 902 °C [7]. The specimen showed no dimensional change or any visible "macroscopic" signs of damage due to this irradiation.

Certain conditions in particular give rise to the amoeba effect. This is where the kernel migrates through the various PyC layers until the particle cracks (as observed with SiC). The Japanese studies have confirmed that with ZrC, no damage is caused when the kernel migrates and comes into contact with the layers, as it is completely stopped.

1.2.3 Properties

ZrC is one of the refractory materials, and it has very useful properties as the result of its composition. The table below compares its properties with those of SiC [8].

Note: these are properties for the material in thin layers, which are somewhat different from those of solid materials. Values are given for normal pressure and temperature conditions.

	Silicon carbide β-SiC	**Zirconium carbide ZrC**
Lattice parameter (Å)	4.358	4.698
Space group	F43m	Fm3m
Composition	SiC	$ZrC_{0.5}$ to $ZrC_{0.99}$
Molar mass ($g.mol^{-1}$)	40.097	104.91
Colour	Yellow to silver-grey if pure. Brown if alloyed with B,N or Al.	Silver-grey
X-ray density ($g.cm^{-3}$)	3.214	6.59
Melting temperature (°C) At 1 atm	2,545 (forms: Si, SiC, Si_2 and SiC_3)	3,420
Heat capacity ($J.mol^{-1}.K^{-1}$)	28.63	37.8
Dissociation enthalpy (-ΔH)	-28.03±2 $kJ.mol^{-1}.K^{-1}$	196 $J.mol^{-1}.K^{-1}$
Thermal conductivity ($W.m^{-1}.°C^{-1}$)	25.5	20.5
Thermal expansion ($10^{-6}.°C^{-1}$)	3.8	6.7
Debye temperature (K)	1,430	491
Supraconducting transition temperature (K)	5	<1.2
Vickers hardness (GPa)	24.5 to 28.2 (varies according to crystal plane)	25.5
Young's modulus (GPa)	475 at 20 °C, 441 at 1.500°C	350 to 440 at 20°C
Shear modulus (GPa)	192	172
Compressibility by volume (GPa)	96.6	207
Poisson coefficient	0.142	0.191
Bending strength (MPa)	350 to 600	-

Table : Comparison of SiC and ZrC properties and characteristics.

1.3 Containment properties

One of the vital properties when selecting a material for the particle coating is its behaviour as a "barrier" to fission products, whether gaseous or solid.

1.3.1 Gaseous fission products

Tests carried out at LASL [7] on TRISO type particles with a $^{235}UC_2$ kernel have shown that ZrC behaves with an integrity comparable to SiC as regards gases (essentially xenon and argon).

1.3.2 Solid fission products

The diffusion of solid fission products such as ^{137}Cs, ^{134}Cs, ^{106}Ru, ^{144}Ce, ^{154}Eu, ^{155}Eu through SiC and ZrC was compared. Particular attention was paid to caesium as it diffuses quickly in carbon and is therefore not stopped by pyrolytic carbon or by the graphite of the moderator. The LASL tests have shown that ZrC and SiC behave comparably as a barrier against ^{137}Cs diffusion. However studies carried out in Japan on TRISO particles with a UO_2 kernel have shown that, unlike Ruthenium, the ^{137}Cs diffusion coefficient is at least 100 times lower in ZrC than in SiC [9],[10].

1.4 Neutron property : transparency

1.4.1 Theoretical transparency calculation

The fact that in-coming and out-going neutrons have different kinetic energy values alters the microscopic absorption cross-section value σ_a for any given atomic nucleus. Given that this parameter is used in calculating transparency, this means calculating the macroscopic absorption cross-section Σ_a for the material in question.
Let X be the atom representing either Zr or Si.
$\Sigma_{a\,XC} = \Sigma_{a\,X} + \Sigma_{a\,C}$
Now $\Sigma_{a\,X} = N_X\,\sigma_{a\,X}$ where N_X is the number of X atoms per cm^3.

$$N_X = N_{XC} = \frac{\rho_{XC}}{M_{XC}} N_A \quad \text{where } \rho_{XC} \text{ is the density and } M_{XC} \text{ the molar mass of compound } XC$$

The following formula is thus obtained for the macroscopic absorption cross-section:

$$\Sigma_{a\,XC} = N_{XC}\,(\sigma_{a\,X} + \sigma_{a\,C}) = \frac{\rho_{XC}}{M_{XC}} N_A\,(\sigma_{a\,X} + \sigma_{a\,C})$$

1.4.2 Transparency to thermal neutrons

Density values

Tables give the following as most probable values for density:
$\rho_{ZrC} = 6.4\ g.cm^{-3}$ and $\rho_{SiC} = 3.21\ g.cm^{-3}$ (for a stoichometric material)

Microscopic absorption cross-section values

In [11], the values given for thermal neutrons at T=25 °C (where velocity v=2,200 $m.s^{-1}$ and hence energy E_c=0.0253eV) are:
$\sigma_{a\,C} = 3.2 \pm 0.2$ millibarns, $\sigma_{a\,Zr} = 0.18 \pm 0.004$ barns, $\sigma_{a\,Si} = 0.13 \pm 0.03$ barns

Numerical values for macroscopic absorption cross-sections

For thermal neutrons at T=25 °C, the calculated values are:
$\Sigma_{a\,SiC} = 5.92 * 10^{-3}\ cm^{-1}$ and $\Sigma_{a\,ZrC} = 6.84 * 10^{-3}\ cm^{-1}$
The transparency values are very close. We can thus say that the neutron properties of ZrC and SiC are comparable as regards transparency to thermal neutrons at a temperature of 25°C.

1.4.3 Transparency to fast neutrons

In this domain (neutrons which energy ranges from 10 keV to 10 MeV), many elements have resonances and the data cannot therefore be tabulated. The data are thus shown as the curves giving the total microscopic cross-section (not the absorption cross-section) as a function of the energy of the incident neutrons. The total cross-section represents both absorption and diffusion cross-sections and is used to characterise the reduction in neutron flow when they flow through any given material specimen. The diffusion cross-section is particularly important for light atoms (H, C, etc.), but it is small, even negligible for other atoms and does not depend on their energy.

For fast neutrons (average energy 2 MeV), still at T=25 °C, the following values are given by the graphs [12]:

$\sigma_{T\,C} \cong 1.7$ barns, $\sigma_{T\,Si} \cong 3$ barns, $\sigma_{T\,Zr} \cong 4.9$ barns

The total microscopic cross-section values calculated are:

$\Sigma_{T\,SiC} = 0.209\ cm^{-1}$ and $\Sigma_{T\,ZrC} = 0.246\ cm^{-1}$

Thus ZrC is slightly less transparent to fast neutrons than SiC.

1.4.4 Influence of temperature on transparency

For elements which effective cross-section varies by 1/v, hence by $1/\sqrt{E_c}$ (neutrons with a Maxwell spectrum), σ varies according to temperature (in K) by a function of the following type:

$$\sigma(T) = \frac{\sigma(T_0)}{1.128}\sqrt{\frac{T_0}{T}}$$

where $1.128 = 2/\sqrt{\pi}$ is a corrective factor for neutrons with a Maxwell distribution.

The microscopic absorption cross-sections of C, Zr and Si have the same function; only Rh, Ag, Cd, In, Te, Sm, Eu, Gd, Er, Lu and Hf do not have this function. For these elements:

$$\Sigma_{aXC}(T) = \frac{\Sigma_{aXC}(T_0)}{1.128}\sqrt{\frac{T_0}{T}}$$

It can be shown that at high temperatures the neutron properties of ZrC and SiC are comparable, and even more so as σ decreases, when temperature increases. In such cases the difference between ZrC and SiC becomes negligible.

II. Comparison of different ZrC deposition processes

2.1 Reactants used

2.1.1 Zirconium precursor gas

Different precursors

To bring zirconium to the reaction, zirconium halides such as $ZrCl_4$, $ZrBr_4$ [13][14], ZrI_4 [15] are used. All three kinds of these precursor gases were used during studies on ZrC coating. The most commonly used methods entailed zirconium chloride ($ZrCl_4$) and zirconium bromide ($ZrBr_4$).

2.1.1.1 Chloride method

In the literature, several methods of $ZrCl_4$ synthesis are described in detail, of which two have been successfully used:

First method: sublimation

$ZrCl_4$ in powder form is used - a product manufactured in industry during Zr metal manufacturing phases. To obtain gaseous $ZrCl_4$, either:

- the powder is heated to temperature T=315°C, close to its sublimation temperature (T= 356°C). $ZrCl_4$ gas formed in this way is diluted by a current of "carrier" gas (argon) and transported to the furnace [16],

- or a distributor is used (see Figure I.1) to carry the powder into a chamber before it is pulverised with argon in the high temperature furnace. Given the low mass of the $ZrCl_4$ in comparison with the mass of the other reactants in the furnace, the powder is sublimed with such low sublimation energy that no change in temperature [17] is observed.

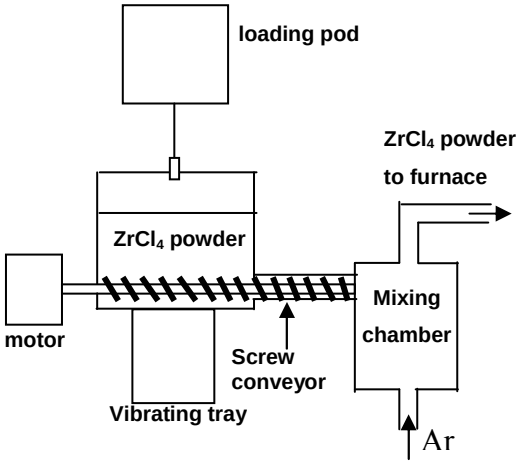

Figure I.1: Powder distributor system used by the Americans [17].

Although these techniques give good results, the main problem they pose is accurately managing the chloride mass flow, whether introduced as a gas or using the screw conveyor. Moreover, handling $ZrCl_4$ in powder form remains delicate operation as a powder tends to clump and it is dangerous in contact with air (HCl released).

Second method: in-situ chlorination

Solid Zr is pickled (sponge, granules, etc.) at temperature in a gas such as Cl_2 or CH_2Cl_2, the latter of which has the advantage of producing both the hydrocarbon to bring carbon to the reaction and the precursor chloride for zirconium. Nevertheless, the worry in this case is that premature carbon deposition should occur on the metal zirconium, thus destroying the metallic support.

Likewise, with chlorination, there is a risk of capturing chlorine ($\sigma_{a\ Cl}$ = 31.1±1.0 barns) as traces in the deposit.

2.1.1.2 Bromide method

The most commonly used method [18][19] to deposit ZrC by CVD using bromide consists of passing argon saturated with bromine at 0°C through zirconium sponges at 600 °C (figure I.2). Given these conditions, almost all the bromine is converted into $ZrBr_4$. The mixture is diluted with hydrogen.

The other option is to use Br_2, which is liquid at room temperature, with argon bubling to vaporise it.

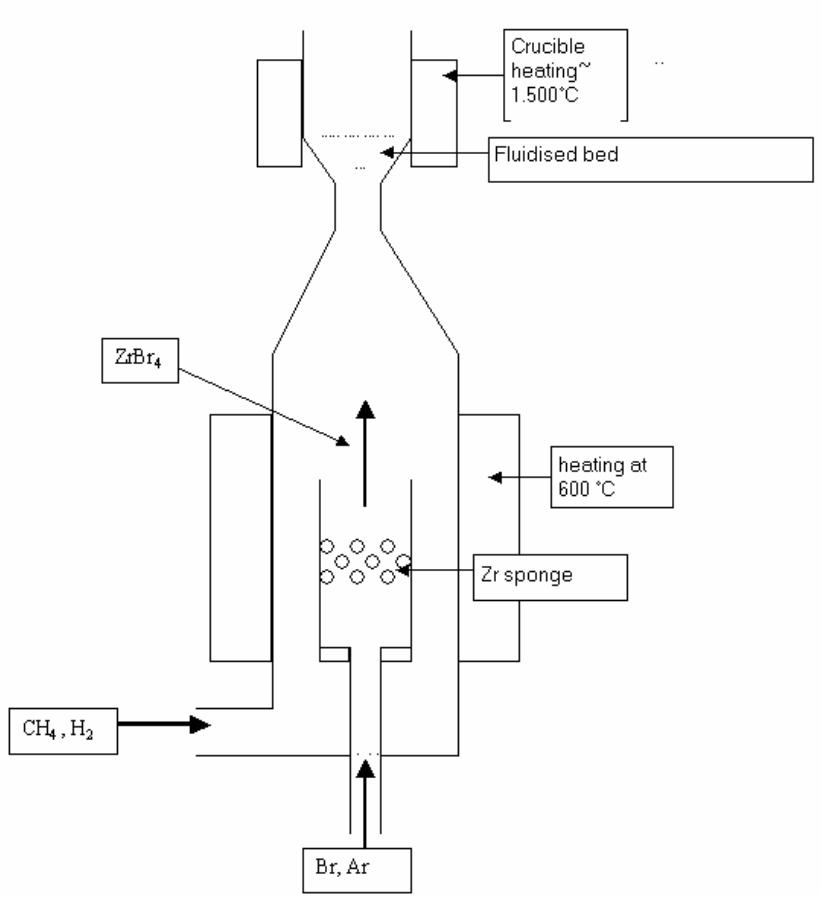

Figure I.2: Diagram of ZrC deposition using bromide installation (JAERI).

It should be noted that whatever precursor and synthesis method are selected, it is vital that the zirconium used has had all hafnium removed, as hafnium is a neutron poison. With a microscopic absorption cross-section of $\sigma_{a\ Hf} = 115 \pm 5$ barns, much higher than that of Zr ($\sigma_{a\ Zr} = 0.18 \pm 0.02$ barns), Hf absorbs incident neutrons. However, hafnium is one of the main impurities in the zirconium ore. It is imperative therefore that Hf < 100 ppm.

2.1.2. Carbon precursor gas

Carbon is generally brought to the reaction by methane CH_4 at high temperature or sometimes propylene C_3H_6 [20]. However, it should be noted that with C_3H_6 the coating rate and the efficiency are lower. This gas is mainly used for pyrolitic carbon deposition or for depositing composite ZrC-C layers [21]. Previous studies [22] have shown that increasing CH_4 and H_2 concentrations can improve coating rates. Increasing CH_4 to halide ratio leads to a less metallic appearance and the ratio of C to Zr increases in the deposition composition. Note that hydrogen can be used to reduce this effect.

2.1.3 Carrier gases

These carriers are:

- argon, a neutral gas which dilutes the zirconium halide and contributes to fluidising the bed of the kernels to be coated,
- hydrogen H_2, a powerful reducing agent which prevents oxide formation, captures chlorine and prevents the formation of free carbon [22].

This is the basis on which the thermodynamic study was carried out, by initially simulating the in-situ synthesis of the zirconium precursor gas and subsequently simulating ZrC deposition by adding another reactant gas.

III Thermodynamic study

The thermodynamic study was carried out at LTPCM (laboratory of thermodynamics and metallurgical physico-chemistry), a laboratory which is supported by the CNRS (French national scientific research centre), the UJF (Université Joseph Fourier) and the INPG (Institut National Polytechnique de Grenoble), based at ENSEEG (national school of electrical industry and electro-metallurgy of Grenoble).

This study was carried out using the SGTE (Scientific Group Thermodata Europe) database. The literature review was used to validate the data in this database. Calculations were made using the Chemsage software in the basis of files in which all data regarding the systems studied were gathered.

3.1 Systems studied

The systems involved are:

→ (Zr-Cl-C-H-Ar) for <Zr> chlorination with HCl, Cl_2 or CH_2Cl_2
→ (Zr-Br-C-H-Ar) for <Zr> bromination with HBr and Br_2
→ (Zr-I-C-H-Ar) for <Zr> iodination with HI

For each system, the study comprises two parts: synthesising the zirconium precursor gas by chlorination, bromination or iodination and ZrC deposition by CVD using the gas obtained, with an added hydrocarbon to bring the carbon to the reaction.

3.2 Literature review

3.2.1 Principles for thermodynamic equilibrium calculations

Chemical deposition of a solid phase from a gaseous phase is a complex process which brings several phenomena such as thermodynamics, kinetics and diffusion into play. We are solely interested in thermodynamic issues. The feasibility of deposition is determined by calculating the equilibriums between the different phases of a chemical system; these calculations are also used to assess the influence of the various experimental parameters on the possible appearance of each phase.

This approach can be used to model tendencies within a chemical system and thus predict the experimental conditions which would favour deposition of the composition in question. It can significantly reduce the time taken to develop a synthesis technique.

The first stage consists of identifying all known species that may be formed during deposition reactions, as well as their stability domain. The table below gives an example of the list of species taken into account for the system (Zr-Cl-C-H-Ar):

Condensed species	Solid solutions: BCC(Zr); FCC(Zr:C); HCP(Zr). Defined compounds: Cgraphite; CCl4; C6ClH5; ClZr; Cl2Zr; Cl3Zr; Cl4Zr; H2Zr
Gaseous species	Ar; C; C2; C3; C4; C5; CCl; CCl2; CCl3; CCl4; C2Cl; C2Cl2; C2Cl3; C2Cl4; C2Cl5; C2Cl6; CClH; CClH2; CClH3; CCl2H; CCl3H; C2ClH; C2ClH3; C2ClH5; C2Cl2H2_1,1C2H2Cl2; C2Cl2H2_CIS; C2Cl2H2_TRANS; C2Cl2H4; C2Cl3H; C2Cl3H3; C2Cl4H4; C2Cl5H; C6ClH5; CH; CH2; CH3; CH4; C2H; C2H2; C2H3; C2H4; C2H5; C2H6; C3H; C3H4_1; C3H6; C3H6_1; C3H8; Cl; Cl2; ClH; ClZr; Cl2Zr; Cl3Zr; Cl4Zr; H; H2; HZr; Zr; Zr2.

The basic principle of a thermodynamic equilibrium calculation based on external variables, temperature T and pressure P, is to minimise the total Gibbs free energy (G) for the chemical system studied. The second stage of the process is thus to establish a consistent set of thermodynamic data to correspond to the species listed above. These data are analytically described using Gibbs free energy functions for each system phase.

3.2.2 Data used

3.2.2.1 Available thermodynamic data

Several databases exist and the choice was therefore made to use SGTE, the most recent database. However, it was important to check whether any of these databases had been criticised, so that the most appropriate database could be selected and, if necessary, additional data added. The thermodynamic data from Van der Vis and Cordfunke [23] were thus used as these authors criticise some data in the SGTE database relating to Zr halides and in particular solid species. After having inserted Cordfunke's solid halide data into the file used by Chemsage and having taken into account the missing species $H_2Zr^{(*)}$ carried over into the Coach database (Thermodata), the chlorination simulation shows that a solid chloride appears (see Figure II.1) and that, whichever data are selected, the same gaseous species are obtained at the end, in particular comparable quantities of $ZrCl_4$.

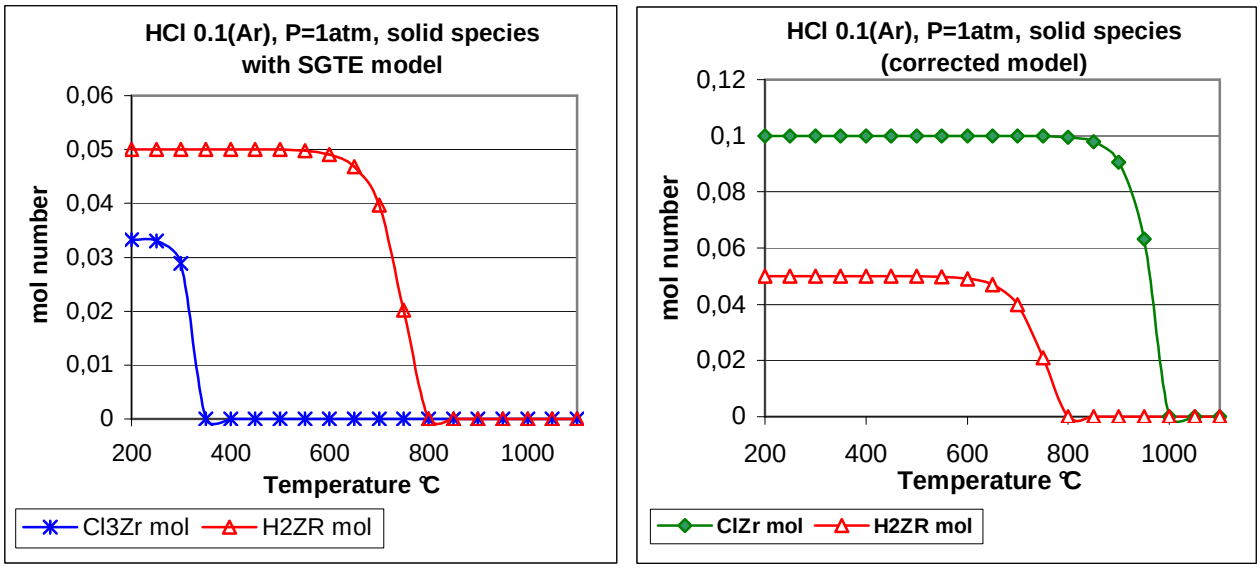

Figure II.1: Comparison of the SGTE model and the corrected model.

(*) The data for H_2Zr were published by O. Knacke and O. Kubaschewski in 1991, citing the International Atomic Energy Agency, Vienna, 1976 as source.

3.2.2.2 Model used for ZrC

The substructure model was preferred to the substitution model [24]. According to the substitution model, it is assumed that the Zr and C species distribution is completely random within the solution formed and that simply by substituting Zr atoms for C atoms, the composition of the solution can vary completely from pure Zr to pure C. This model thus describes the liquid phase as a binary relationship between Zr-C but does not properly represent the domain which is the solid in solution. On the other hand, with the substructure model, the solid solution Zr_xC_{1-x} is broken down into two substructures each comprising two elements. One is filled with Zr and C atoms and the other is partially full of Zr atoms in interstitial position, with the species considered as a further chemical species. The corresponding formulation is thus $(Zr,C)_a(Zr,Va)_c$, where a and c are coefficients giving the sites in each substructure and, in this case, as ZrC is a CFC phase, we have a=b=c=1. The limits of the ZrC single-phase domain are calculated like so and the curves obtained are then checked to see whether they are close to the experimental graphs, which would confirm that the model selected is appropriate (see Figure II.2).

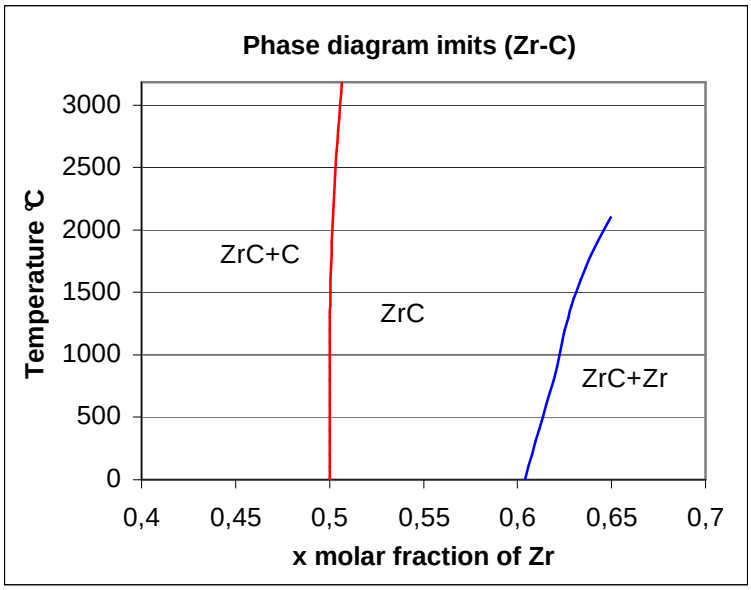

Figure II.2: Calculation of the phase diagram limits.

3.3 Simulation of halidation and CVD deposition stages

First of all, the simplified assumptions on which the simulation is based must be clearly stated. It is assumed that:

- thermodynamic equilibrium is achieved. This hypothesis is close to reality for deposition reactions as furnace temperatures are greater than 1,000 °C, which can give rise to fast kinetics,
- the reactor is a closed system unlike the experiment conditions in which deposition takes place under a continuous gas flow.

3.3.1 Simulation of the Zr halidation stage

This stage is carried out via a flow of gaseous halide (diluted or otherwise with argon or hydrogen) which is passed through a Zirconium bed (sponge, granules, etc.). The composition of the various gaseous and solid products resulting from the reaction at equilibrium is found via a simulation using the following assumptions:

- there is excess metal as compared to the gaseous halide, i.e. there is a total reaction between the gas introduced and the Zr solid load,
- this gas stays for an infinite period of time within the reactor.

The simulation is run for a large range of temperatures (250°C<T<450°C) in order to analyse the influence both of pressure and of the dilution in Ar or H_2 of the gaseous halide selected for the synthesis of the Zr precursor gas.

3.3.2 Simulation of deposition stage

In practice, the following are injected to the CVD furnace:

- all gases from the previous stage,
- C precursor gas (CH_4 or C_3H_6),
- argon, diluting gas for fluidising the particle bed,
- hydrogen, in the knowledge that this is also one of the halidation products (HCl, CH_2Cl_2, HBr and HI).

The initial conditions thus include the Zr, CH_4 or C_3H_6 precursor gases, Ar and H_2, whose partial pressure is given by the equation:

$$P = P_{Zr\ precursor} + P_{CH4} + P_{Ar} + P_{H2}$$

where P is the total pressure.

The Zr_xC_{1-x} stoichometric lines are drawn for x=0.51 and x=0.55 on the deposition graphs obtained, along with the limits of the ZrC-C and Zr-ZrC domains, according to the initial partial pressure of the Zr and C precursor gases. To do this, the limits are found on the graph (see Figure II.3) and successive dichotomies are used to identify the values more accurately.

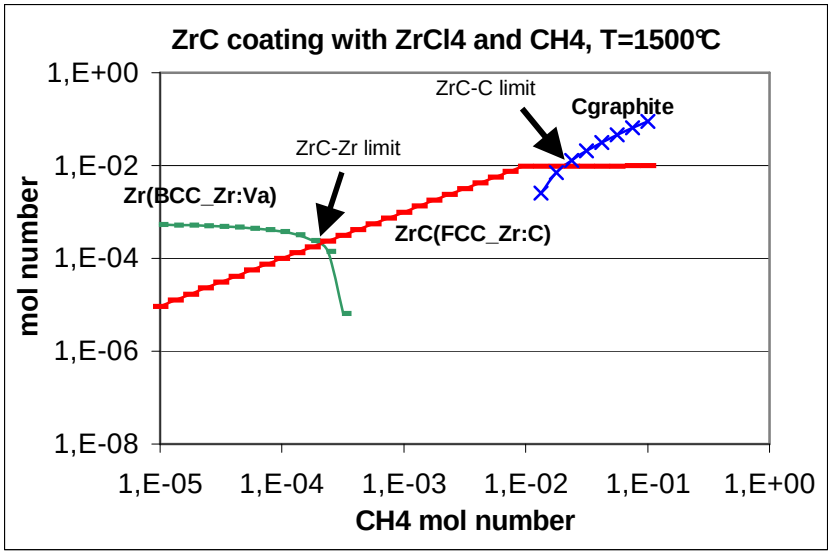

Figure II.3: Solid species that appear at deposition (with chlorination).

3.4 . (Zr-Cl-C-H-Ar) system

3.4.1 Simulation of chlorination

3.4.1.1 The different stages of chlorination

A gaseous mixture containing the chlorine precursor is reacted with excess zirconium.

At low temperatures, it is mainly solid chlorides and hydrides that are formed. The gaseous species (mainly $ZrCl_4$) only form at approximately 600 °C and above. This result suggests that in a steady state, the gaseous halide reacts with the solids formed (ZrCl and ZrH_2) to recover the Zr load. Simulating this process is thus a question of simulating the initial gaseous mixture with these solid species. Gaseous $ZrCl_4$ is thus obtained without any other sub-chlorides (see Figure II.4).

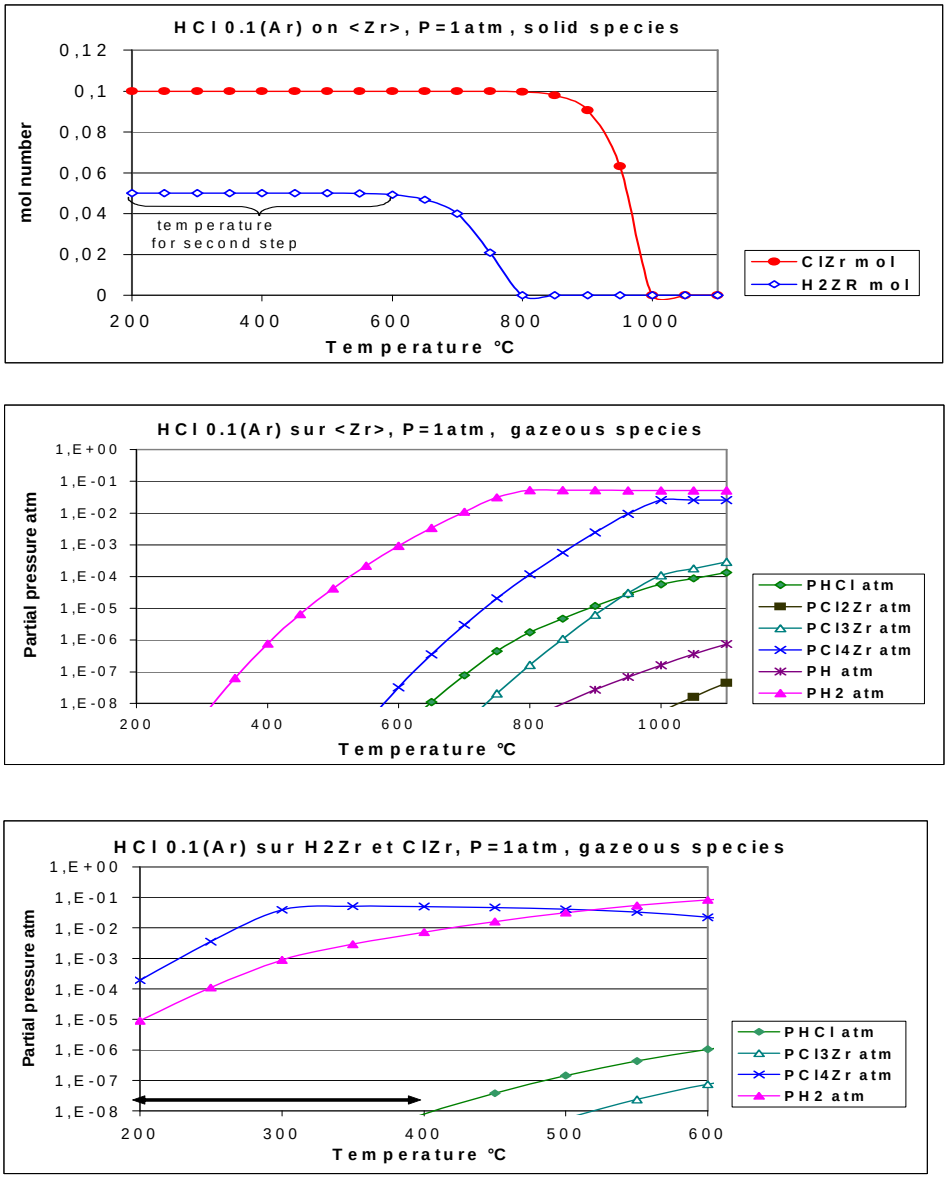

Figure II.4: Procedure followed for simulating Zr precursor synthesis.

3.4.1.2 Comparison of different chloride precursors

As could have been predicted, Figure II.5 shows that Cl_2 gives a better yield than any other chlorinated gas. But for safety reasons, the study will now focus on HCl, which is less dangerous to handle (less toxic and inflammable) than Cl_2.

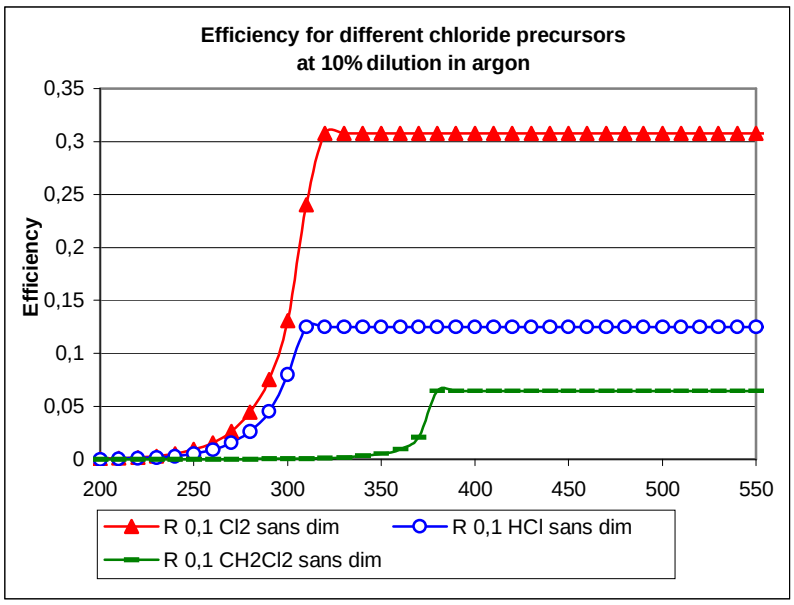

Figure II.5: Yields with HCl, Cl_2 and CH_2Cl_2 at 10 % dilution in Ar.

3.4.1.3 Influence of the various parameters

→ Total pressure

It can be seen from Figure II.6, that at T=250°C, the optimum total pressure to obtain a maximum quantity of gaseous $ZrCl_4$ is 0.1 atm. However, at T=450 °C, between 1 and 10 atm are more useful values. At a mean temperature of 350°C, working at atmospheric pressure thus seems appropriate.

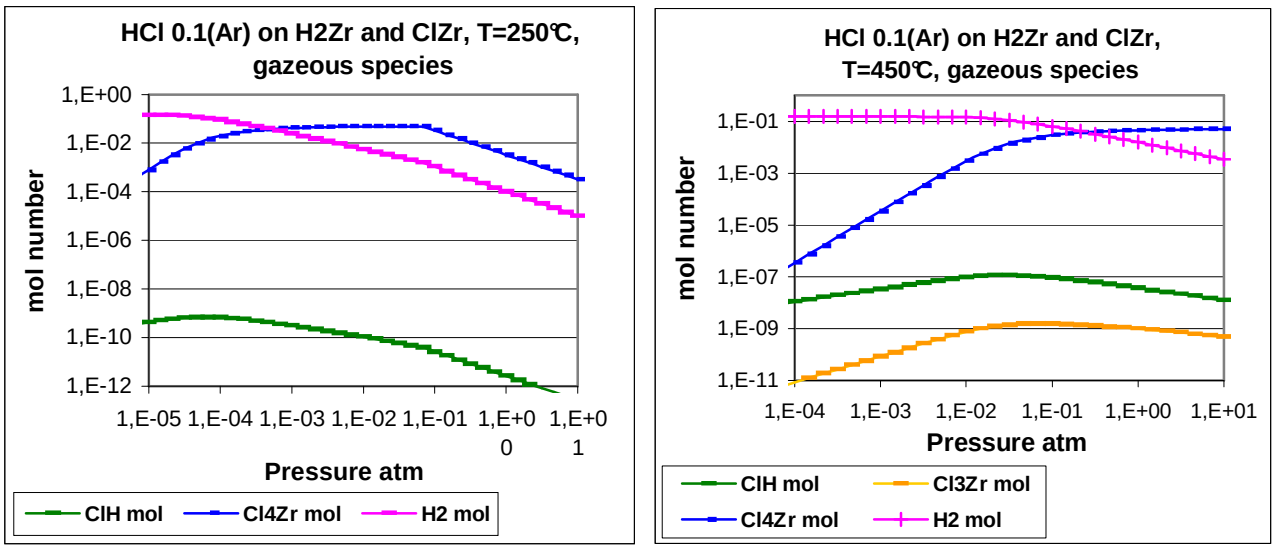

Figure II.6: Influence of pressure on chlorinator temperature limits.

→ Dilution in argon or hydrogen

The first graph (see Figure II.7) shows that, for HCl heavily diluted in argon, the maximum yield can be obtained at 300 °C.

On the second graph, it can be seen first of all that with the mixture of HCl and H_2, no gaseous species are formed at temperatures lower than 387 °C, and consequently no gaseous $ZrCl_4$. This means that higher temperatures need to be used. Moreover, the best yield is gained with HCl diluted with smaller amounts of argon.

If HCl is used, it would appear preferable to dilute it heavily with argon and carry out chlorination between 300 and 350 °C.

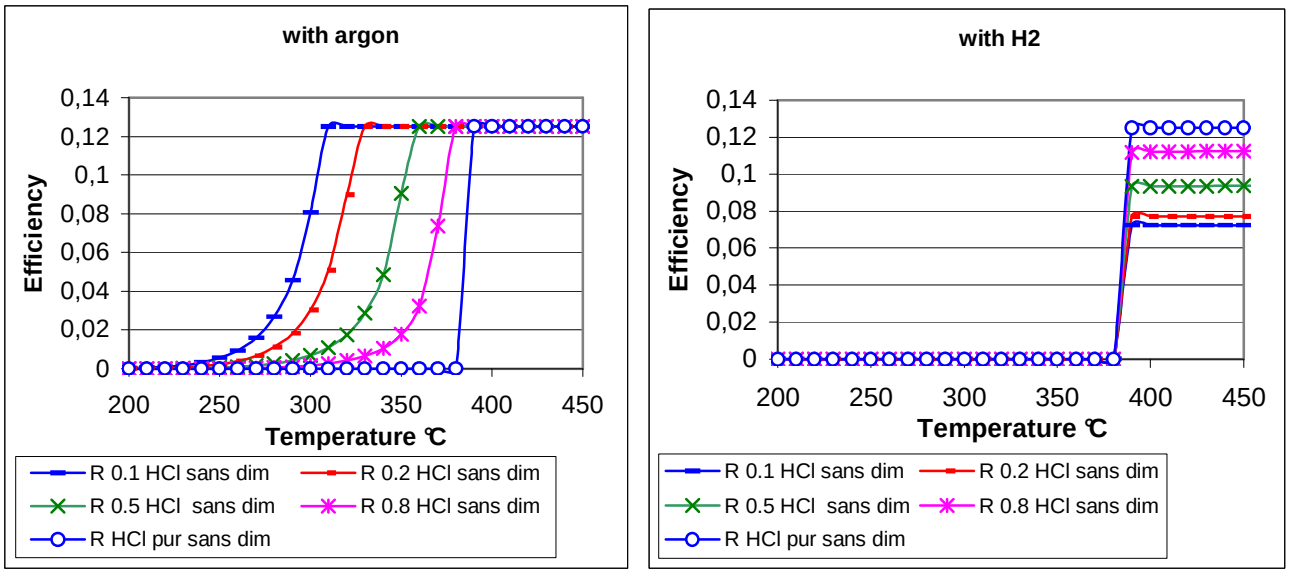

Figure II.7: Influence of HCl dilution in Ar and H_2.

3.4.2 Simulation of ZrC coating

3.4.2.1 Deposition graphs

The graphs (see Figure II.8) give the partial pressure values for CH_4 and $ZrCl_4$ that need to be targeted in order to give a perfectly stoichometric ZrC deposition, that is between the curve on the limit of the ZrC-C and ZrC domains (x = 0.5) and the stoichometric line x = 0.51. As temperature increases, the stoichiometric ZrC coating domain tends towards the higher pressure values. A high temperature is thus more appropriate as the partial temperatures required are within the ranges imposed by the gas supply. The experiments could thus be initiated at an intermediate temperature of 1,600°C.

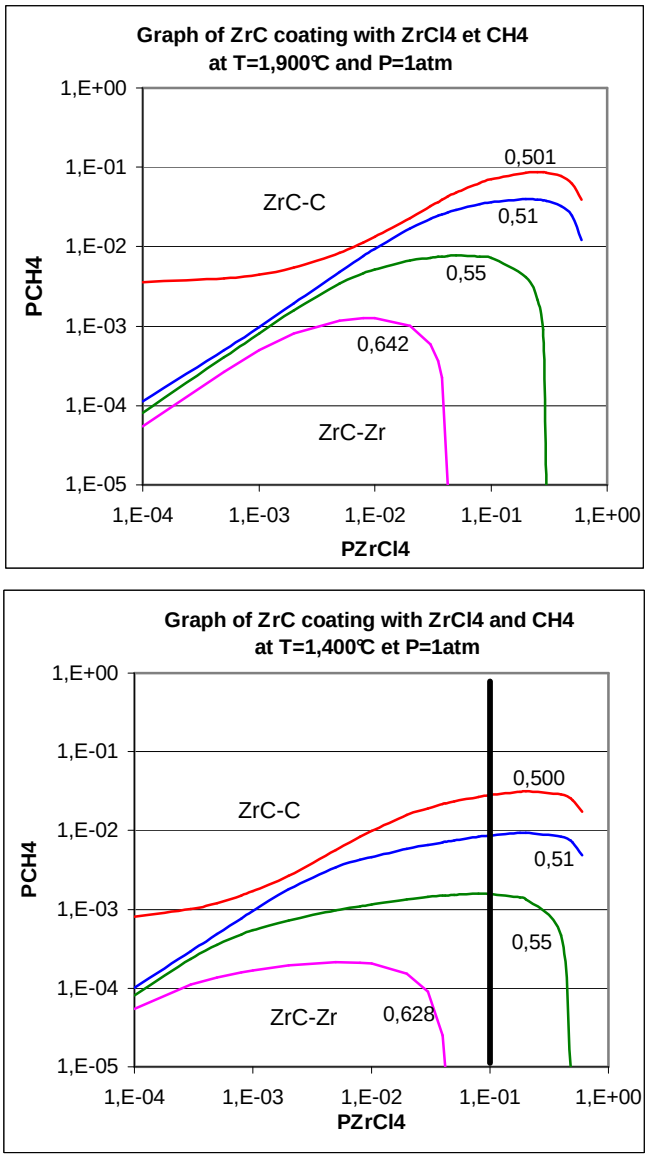

Figure II.8: Graphs of ZrC coating at T=1,400 and 1,900 °C.

3.5 (Zr-Br-C-H-Ar) system

3.5.1 Bromination with HBr or Br_2

As with chlorination, there are two stages in this process: an initial stage during which the solid species are formed (BrZr and H_2Zr for HBr; BrZr alone for Br_2) and the subsequent stage in which gaseous $ZrBr_4$ is mainly formed.

Figure II.9 shows that using heavily diluted HBr is more effective. A better yield is obtained with Br_2 than with HBr.

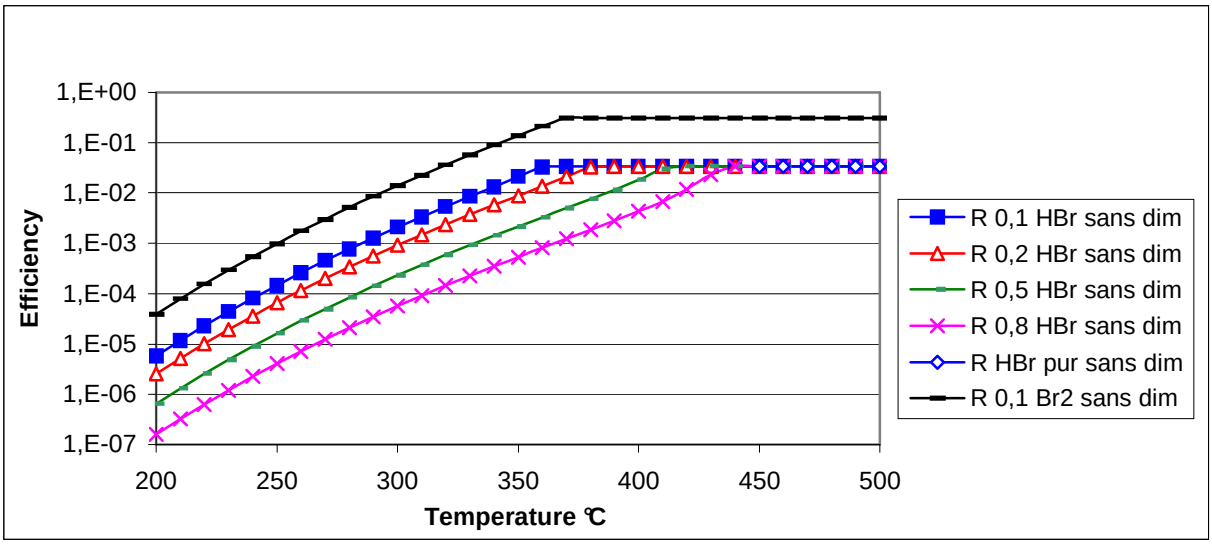

Figure II.9: Efficiency with different dilutions of HBr and Br_2 in argon.

The graph in Figure II.10 for the deposition stage with $ZrBr_4$ and CH_4 is comparable with the graph obtained using $ZrCl_4$.

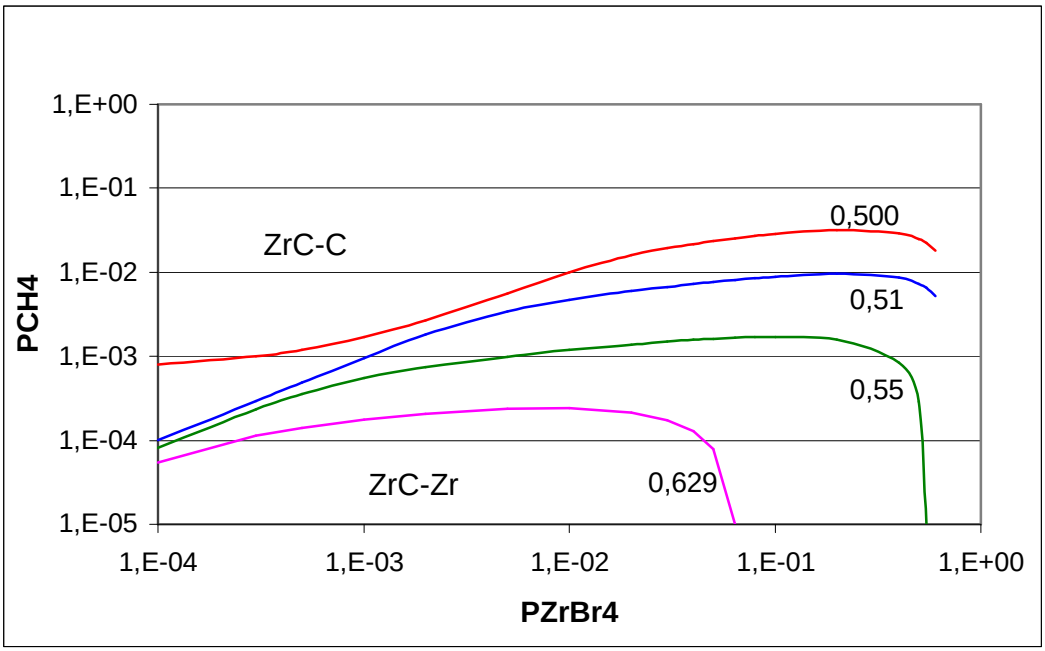

Figure II.10: Deposition graph using CH_4 and $ZrBr_4$ at T=1,400 °C and P=1atm..

3.6 (Zr-I-C-H-Ar) system

As with chlorination, it can be seen that with iodination, it is solid species (IZr and H_2Zr) that initially form, then subsequently ZrI_4 is mainly formed.

However, the yield obtained is low, whatever the dilution (see Figure II.11). The solution would be to carry out synthesis at higher temperatures, but the technical capacity to do this does not exist.

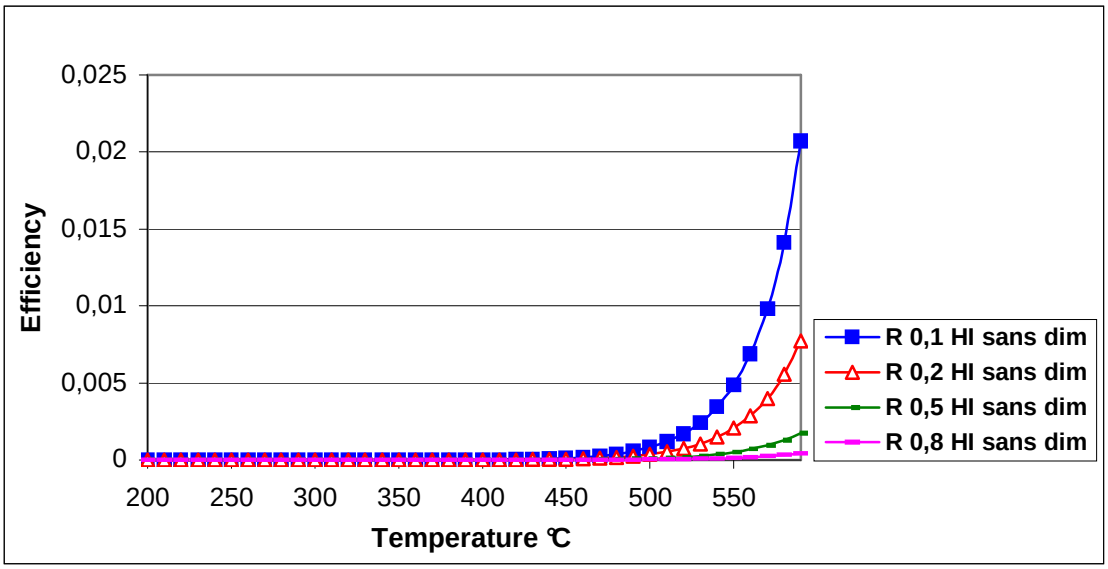

Figure II.11: Efficiency with different dilutions of HI in Ar.

As regards ZrC deposition using ZrI_4 and CH_4 (Figure II.12), these stoichometric lines obtained upon simulation tend towards the higher partial pressure values for CH_4.

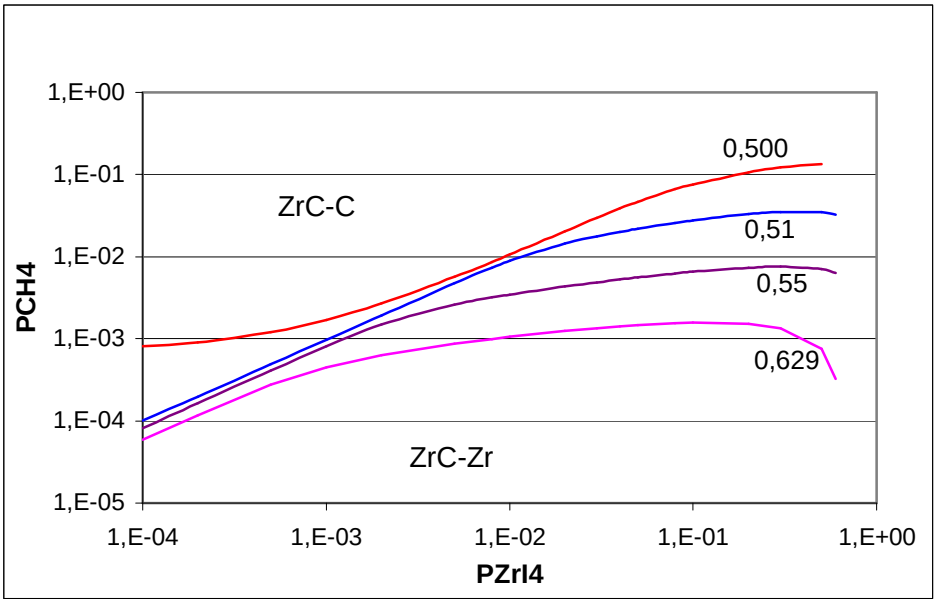

Figure II.12: Deposition graph using CH_4 and ZrI_4 at T=1,400 °C and P=1 atm.

3.6.1 Comparison of the methods

The tables below show the thermodynamic yield values for the chloride and bromide methods for different flow rate and temperature conditions.

- Chloride method

T(℃)	$PZrCl_4$(atm)	flowrate$ZrCl_4$(L/mn)	PCH_4 (atm)	flowrateCH_4(L/mn)	yield
1,400	0.01	0.3	0.008	0.24	70 %
1,400	0.1	3	0.02	0.6	20 %
1,500	0.01	0.3	0.007	0.21	70 %
1,500	0.1	3	0.03	0.9	25 %
1,600	0.01	0.3	0.01	0.3	100 %
1,600	0.1	3	0.03	0.9	35 %
1,900	0.01	0.3	0.01	0.3	100 %
1,900	0.1	3	0.07	2.1	60 %

- Bromide method

T(℃)	$PZrBr_4$(atm)	flowrate$ZrBr_4$(L/mn)	PCH_4(atm)	flowrateCH_4(L/mn)	yield
1,400	0.1	3	0.02	0.6	20 %
1,400	0.01	0.3	0.01	0.3	80 %
1,600	0.1	3	0.05	1.5	40 %
1,600	0.01	0.3	0.01	0.3	100 %
1,700	0.1	3	0.1	3	100 %
1,700	0.01	0.3	0.01	0.3	100 %
1,900	0.1	3	0.08	2.4	100 %
1,900	0.01	0.3	0.09	2.7	100 %

The thermodynamic study has shown that with methane, the theoretical efficiency with the bromide method is, on average, higher for Zr, before free carbon appears.

Previous studies have also looked into this method which can give a stoichiometric ZrC deposition in a wide range of working conditions (temperature and flow rate with different gases) [25]. When deposition uses bromide, the methane controls the deposition rate and the $ZrBr_4$ controls the stoichometric ZrC conditions.

However, there are technical drawbacks to this method. Bromination must be carried out at 0°C and it is generally easier to heat (or trace) components that to cool them down. Moreover, although HCl is considered a hazardous gas, bromine is even more toxic.

For our tests, it was decided to use chlorination by a mixture of HCl diluted in argon, injected in conjunction with C_3H_6 or CH_4 if possible and pre-heated.

3.7 Composition of the gaseous phase

Figure II.13 shows that many gaseous species, hydrocarbons and sub-chlorides are formed upon deposition and that consequently, the gaseous precursors CH_4 and $ZrCl_4$ injected into the furnace do not react fully to form ZrC.

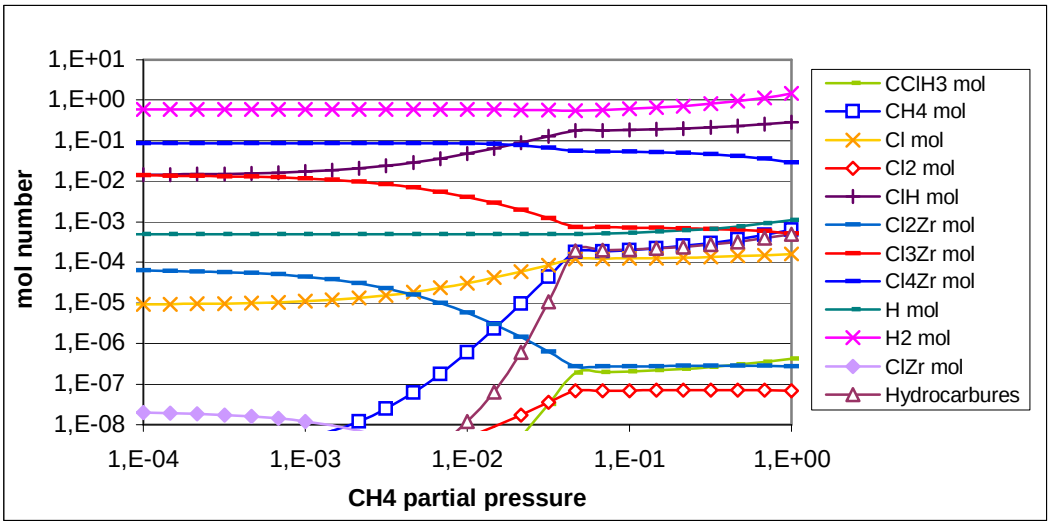

Figure II.13: Composition of the gaseous phase at T=1,600°C and P_{ZrCl4}=0.1 atm.

3.7.1 Zr and C efficiencies in compounds at equilibrium

In order to obtain perfectly stoichometric ZrC, it is important to be at the point just before free carbon appears. Figure II.14 shows that, in this case, the C yield in the ZrC is 98 %, whereas the Zr yield in the ZrC is only 40 %. Unlike $ZrCl_4$, therefore, CH_4, is totally cracked to form ZrC.

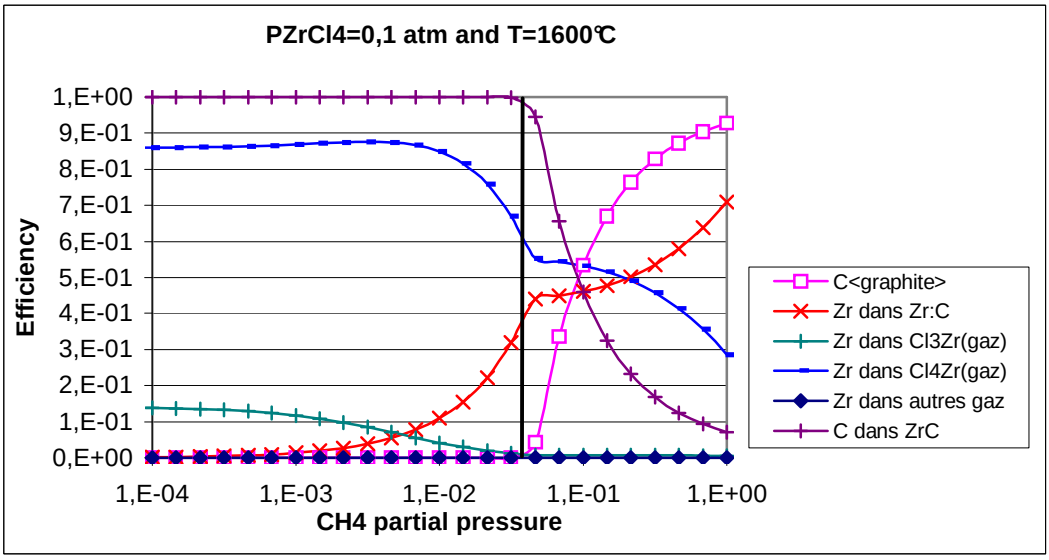

Figure II.14: Zr and C efficiencies in the main compounds.

3.7.2 Comparison of C precursors: CH_4 and C_3H_6

The graphs in Figure II.15 show that under identical temperature and pressure conditions, the stoichometric ZrC deposition domain tends towards lower partial pressures when C_3H_6 is used. However, one might think that the difference at equilibrium would be smaller for depositions using C_3H_6 than deposition using CH_4, which is renowned for its high chemical stability. It is a saturated

species as all four C bonds are simple bonds and it therefore breaks down less easily than the thermodynamic studies predicted.

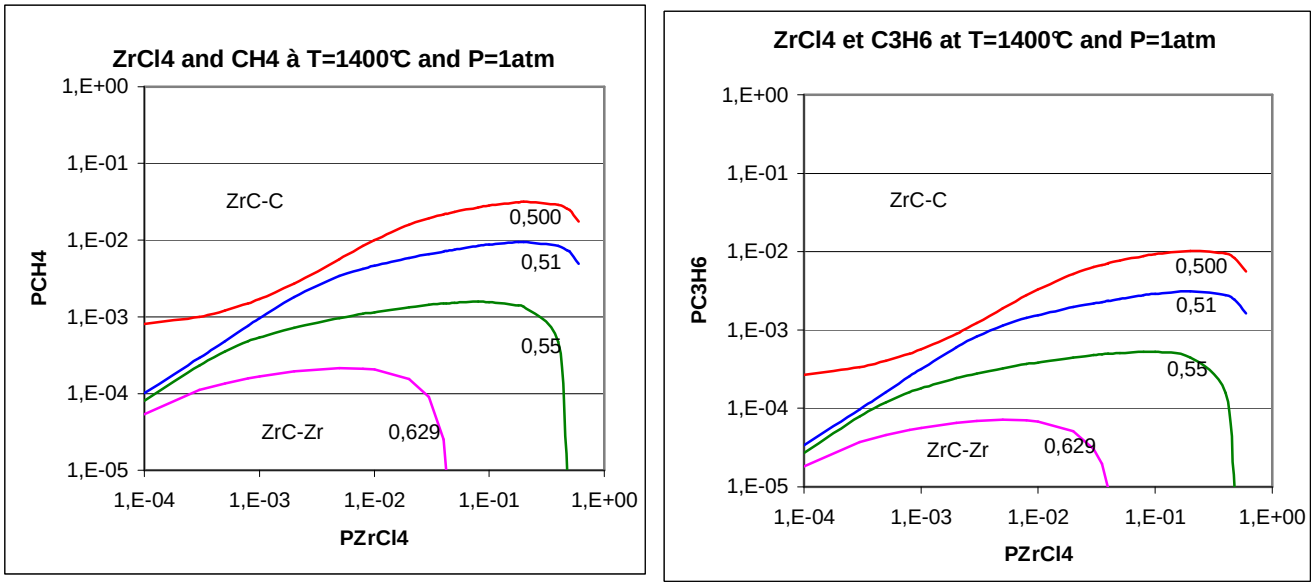

Figure II.15: Comparison of deposition graphs for CH_4 and C_3H_6.

3.7.3 Calculating $ZrCl_4$ condensation temperature

Prior to the experimental phase, it was important to check $ZrCl_4$ stability at a cold point. The condensation temperature for gaseous $ZrCl_4$ produced by chlorination with a mixture of HCl (10 %) and Ar, is given by the $ZrCl_4$ saturated vapour pressure at a given temperature and pressure. Hence it depends on the conditions in which chlorination takes place. With a partial pressure of gaseous $ZrCl_4$ (P_{ZrCl4} = 0.1095 atm) occurring at T=350°C and P=1atm, the condensation temperature calculated is $T_{condensation}$= 300°C (see Figure II.16). It will thus be important to keep the chloride at a temperature greater than 300°C from the moment of its synthesis right up to the deposition furnace.

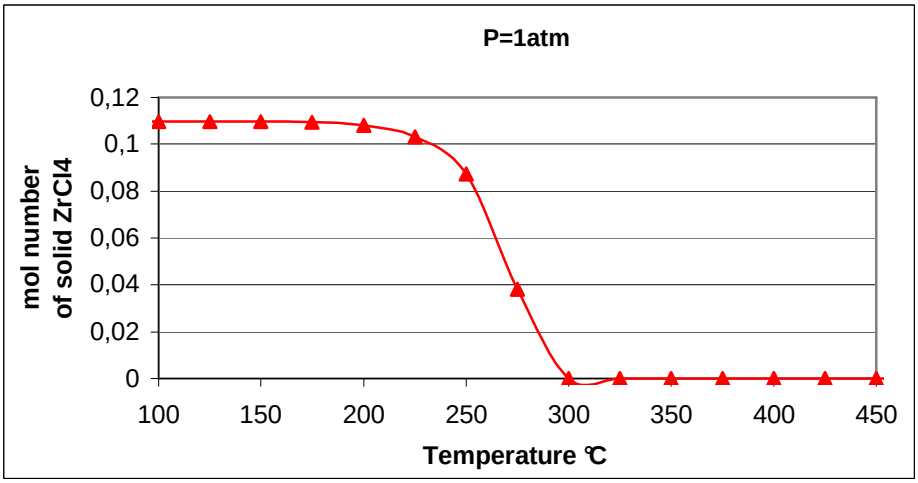

Figure II.16: Condensation of the $ZrCl_4$ formed during chlorination.

IV. Experimental techniques

4.1 Equipment and apparatus

4.1.1 CVD in a fluidised bed: deposition principles

The substrate is made up of perfectly spherical, calibrated kernels of Yttrium stabilised zirconia, forming the bed. They are set in motion by injecting a gaseous mixture of argon, hydrogen and the various gaseous precursors of the products to be deposited, by means of a 3-inch diameter graphic crucible. As the yield is not complete, soot and chlorinated gases produced by the reaction are extracted, filtered and cleaned in a wash column prior to release into a chimney stack.

4.1.2 Chlorinator

4.1.2.1 Apparatus

The apparatus comprises three ventilated chambers (see Figure III.1). The chlorinator is a stainless steel enclosure containing granular zirconium heated to 350 °C by means of two resistors. HCl gas is supplied from a cylinder located in an adjacent chamber, as a safety precaution. The chlorine synthesis reaction takes place within the chlorinator:

$$Zr + 4HCl \rightarrow ZrCl_4 + 2H_2$$

According to the safety sheet, hydrogen chloride is toxic if inhaled, very corrosive, non-flammable and has a suffocating odour. In gaseous form, it is heavier than air (d=1.3). Zirconium, on the other hand, is only slightly toxic. However, any friction or impact must be avoided, given its tendency to combustion. It must be handled in a neutral atmosphere to avoid ignition. Transferring it into the chlorinator required use of a glove box with an argon atmosphere. 25 kg was transferred.

The electrical cabinet and the gas management system (argon for dilution and HCl) are located in the same assembly. Pressure and temperature values are monitored and shown on displays.

Figure III.1: Chlorination apparatus.

The gases are transported from chlorinator output via lines heated up to 400°C by means of resistor wires, to the washing apparatus for gas extraction, or to the reactor. The other gases, H_2, hydrocarbons and argon used for fluidisation are heated to 370 °C and then mixed with the chloride in the injection pipe at the furnace base. Valves are used to determine the gas direction during heating, deposition and extraction at the end of the process. Gases that are not transported to the reactor are taken to the wash column in order to neutralise the chloride gases. All stages of the process (apart from H_2) are controlled by a control unit.

4.1.2.2 Operating method

The chlorinator and the gas lines are heated to between 350 and 400 °C with a gentle argon flow (0.5 l/mn). The CVD furnace is then heated to the required deposition temperature (1,400-1,500°C). Argon must be supplied at a rate of 5 l/mn for a 15-minute period in order to ensure that temperatures (lines, chlorinator) are homogeneous. After this period, HCl injection can begin to start the chlorination. Whilst the chlorine flowrate is being stabilised and up to the set point, gas is extracted by the vent. Once the temperatures and flowrates have been stabilised, injection can take place via the injection pipe into the reactor. After the deposition phase, which lasts between 2 and 3 hours, chloride injection is stopped (HCl flow stopped). The lines are rinsed with nitrogen each time, which is extracted via the vent.

4.2 Characterisation techniques

Laser diffraction particle size analysis is used to measure the thickness of the layers by comparing the diameters before and after deposition.

ZrC density cannot be measured by floatation as SiC could.

→ the shells cannot be separated from the other layers of pyrolytic carbon (PyC) for simple air treatment as the ZrC would become completely oxidised in these conditions,

→ we do not know any liquid which is both dense enough and clear, the conditions required for this method.

However, researchers at the JAERI (Japan Atomic Energy Research Institute) [25] have developed a technique using plasma oxidation to oxidise the outer layer of PyC. The transition can be observed by means of the plasma colour change from pale blue to pale purple when the ZrC is attacked. Given the volume (determined by particle size analysis) and the weight before and after plasma oxidation, a density calculation can be made.

This technique also enables the purity of the material to be checked, in particular the amount of free carbon, which oxidises at a very different rate to that of bonded carbon.

The other method that is used is probably harder to implement. It suggests that the (PyC/ZrC) layers should be calcined. Measurements of the reaction products ZrO_2 and CO_2 are used to find the quantity of free carbon in the ZrC deposition by calculating the difference with the quantity contributed by the pyrolitic carbon.

V. Experimental trials

5.1 Perfecting the gas injection pipe

The first deposition trials highlighted a problem in the gas injection pipe; the temperature was too low for $ZrCl_4$ transport. Indeed, the synthesised chloride condensed and created a blockage. The experiment had to be stopped after 3 minutes as the chlorinator pressure had increased above the

level set by the European standard, at 500 mbar. For reference, condensation temperature at working pressure is 250 °C.

These problems meant that a new pipe had to be designed to reduce the thermal bridge between the cool pipe and the gas injection tube.

• The first chlorine injection test was carried out with the first generation pipe (pipe I) and the chloride condensed in the central tube. The thermal profile of the central gas measured along the pipe with and without gas pre-heating showed that there was insufficient insulation (see Figure IV.1 curves with pipe I hot and cold).

• A second generation pipe (Pipe II) was manufactured in order to give maximum insulation for the central gas in the cooling circuit.

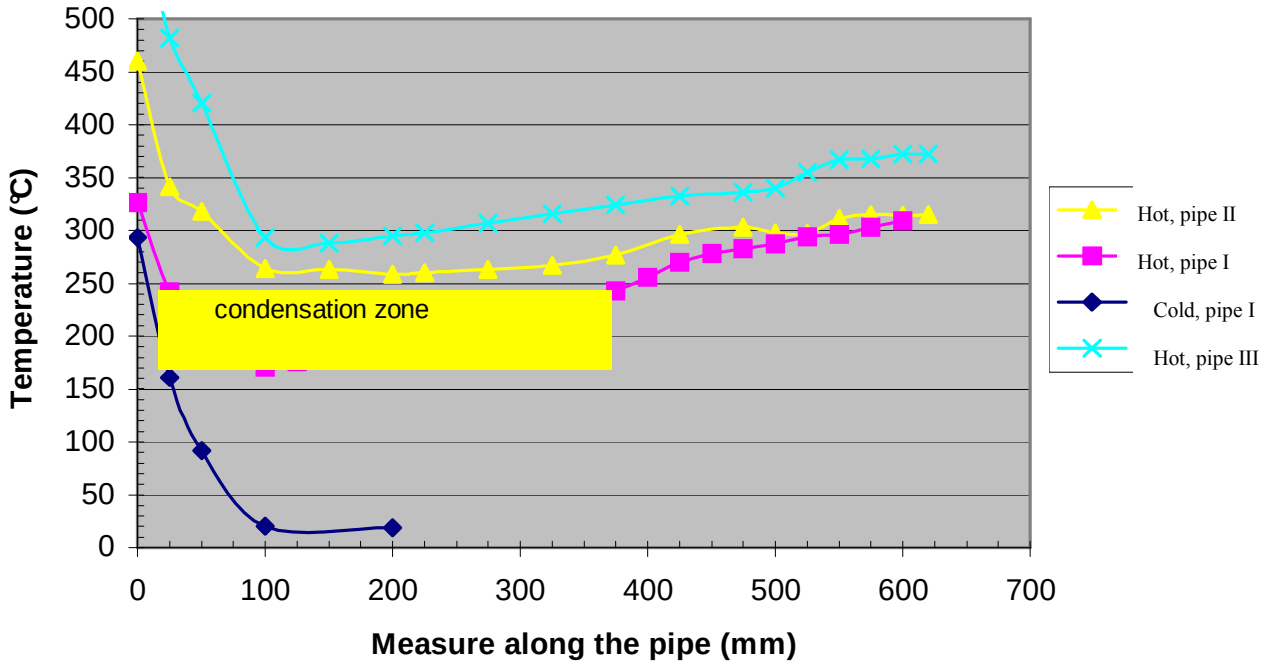

Figure IV.1: Thermal profile of the gas in the injection pipe.

It should be noted that the pipe tip is still cooled by contact with crucible. Moreover, two functionalities were added to the pipe:

- ✓ injector height adjustment,
- ✓ pipe height adjustment.

A thermal profile was carried out on this new pipe (see Figure IV.1, curve for pipe II hot). The thermal loss on input is lower than with pipe I. The minimum temperature is above the $ZrCl_4$ condensation point, but by a fairly slender margin (15 °C).

The injector temperature (460 °C) is higher than with pipe I, probably due to better insulation of the gas tubes, which thus lose less heat, and to the fact that the injector is less exposed to water-cooled walls.

• Given these observations, a third pipe was designed, with the aim of checking whether the central injection tube temperature could be increased after:

- ✓ using lagging to improve insulation of the lower pipe section,
- ✓ altering the outer injection tube length.

The temperature profile (Figure V.1, curve with pipe III hot) for this pipe shows that:

- ✓ the pipe input temperature is 372°C. The minimum temperature in a tube is 288 °C, instead of 260 °C. The input temperature has been increased by 57 °C and the coolest point by 28 °C,
- ✓ the injector temperature is 600 °C (instead of 300 °C at the same point without gas heating and 460 °C for the previous trial),
- ✓ the water flowrate is sufficient, with a low input/output delta T (approx. + 5 °C).

The part of the pipe facing the resistor also had to be insulated. In fact, the thermodynamics seem to require deposition temperatures of around 1,500 °C in the heating area.

5.2 Discussion prior to the deposition trials

The injector temperature increased significantly during these trials. It is not clear whether these depositions can be reproduced for full coating (TRISO) if such a pipe design were to be used. Indeed, a relatively high temperature in the injector could have a number of consequences:

- possible reaction between the gases in the injector after deposition,
- increased pressure drop at nozzle opening.

The use of the outer tube seems to provide good regulation for the thermal loss all the way along the tube (constant power loss along a whole length until sudden heating due to injector).

A temperature of 288 °C is suitable for a mixture which condenses between 240 and 250 °C and so the target has been met.

Even with these results, however, it was important to check that the new pipe design can provide satisfactory deposition of:

- ▪ pyrolitic carbon without premature hydrocarbon decomposition then deposition in injector as a result of the relatively high injector temperature,
- ▪ zirconium carbide : the main issue is the ability to be able to simultaneously inject zirconium chloride and propylene for enough time, without blockage forming, in order to obtain the desired deposition thickness (35 µm) for the application.

5.3 ZrC deposition trials

The kernels are initially covered with two layers of pyrolitic carbon, the first porous (buffer) and the other dense (Inner PyC). We used this trial to check whether the injection pipe behaved correctly:

- no blockage during a sufficiently long trial period (~ 2 hours),
- the feasibility of introducing pre-heated gases without hydrocarbon breakdown in the injector.

However, an excessive temperature increase (> 600 °C) in the chlorinator proved problematic in the final deposition phase. The HCl flowrate was reduced in order to reduce this phenomenon. The propylene flowrate was also reduced to the lowest setting on the flowmeter, which led to an increase in deposition time.

In the end, the particles were covered with dense PyC (Outer PyC), to complete the architecture of the TRISO particles.

5.4 Deposition characterisation

5.4.1 SEM examinations

Intact particles and some whose layers were partially broken were examined (see Figure IV.2). The macroscopic observations made using the scanning electron microscope showed the morphology of these particles, sampled after the ZrC deposition phase. They are sized around 800 µm, and made up of a zirconia kernel measuring approximately 680 µm in diameter, a first layer of porous pyrolitic carbon of 80µm, followed by a layer of dense pyrolitic carbon of 25 µm and a coating of zirconium carbide of approximately 35 µm. It should be noted that the dense PyC and ZrC layers bonded well, as shown by a clean, non-diverted break at the PyC/ZrC interface.

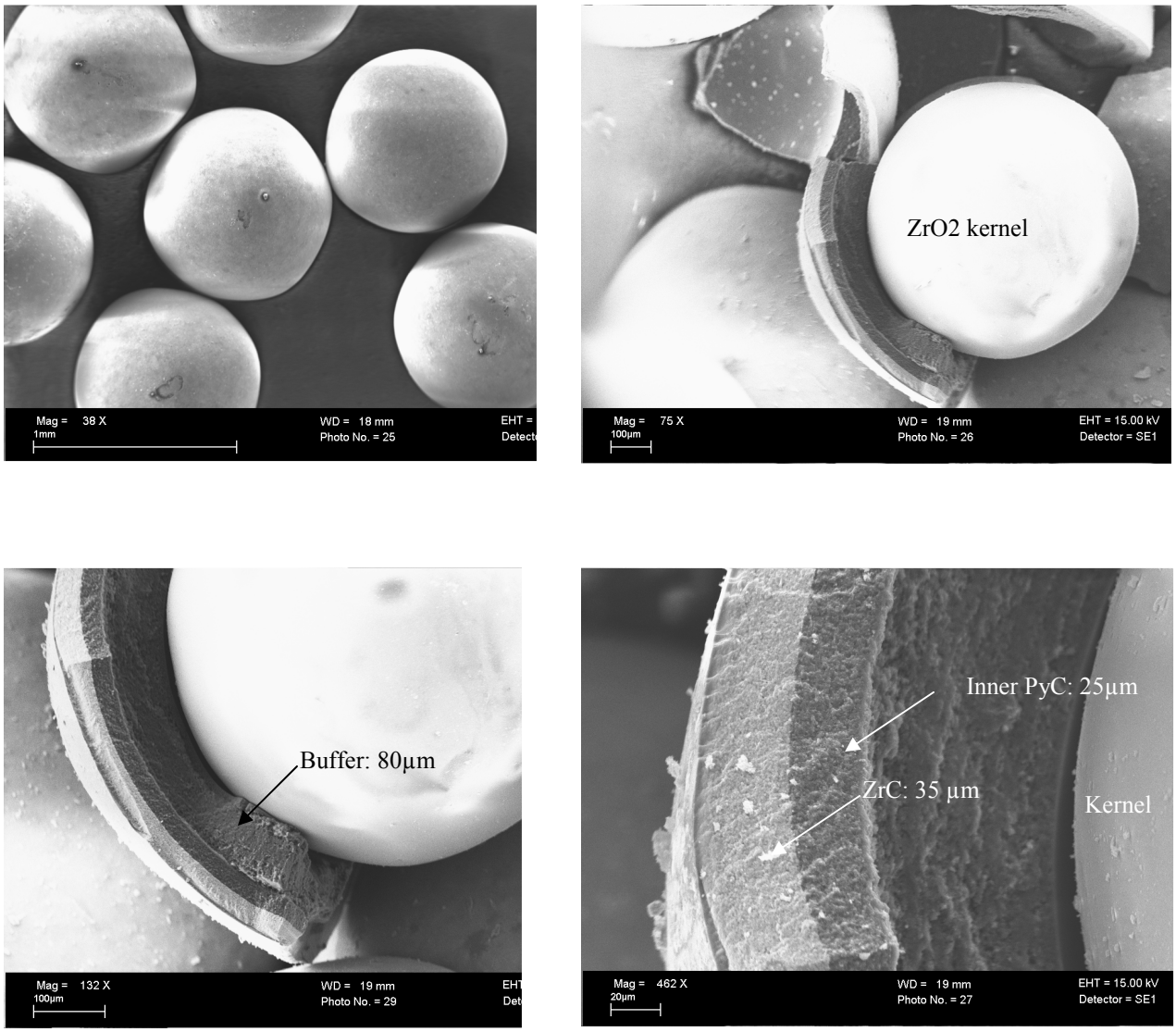

Figure IV.2: SEM observation of particles with no outer PyC after fracturing.

5.4.2 X-ray diffraction examination

These analyses (see Figure IV.3) were carried out on a ground powder. The spectrum reveals ZrC peaks on the cubic-shaped surface layer (a=b=c= 4.693 Å), and also ZrO_2 and ZrO. These data need to be cross-checked with the local chemical data obtained by electron microprobe.

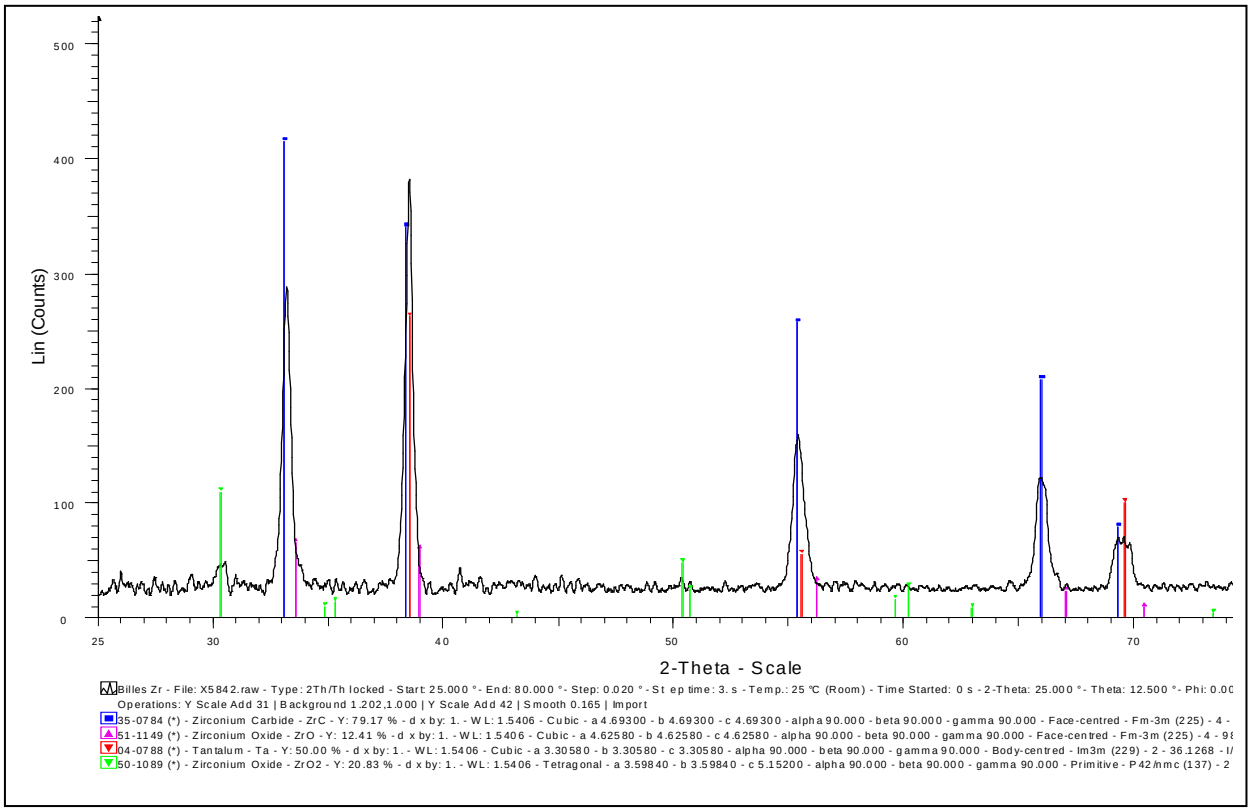

Figure IV.3: Deposition spectrum obtained by XRD.

5.4.3 Polished section examinations

The polished section observations under optical microscope (see Figure IV.4) clearly show the difference in microstructure to correlate with chemical composition gradients in the thickness of the ZrC layer. At the surface, over a thickness of approximately 8 µm, the layer appears compacted but laminated. Deeper in, the layer is granular, with slight variations in colour which highlight either variations in chemical composition or grain size.

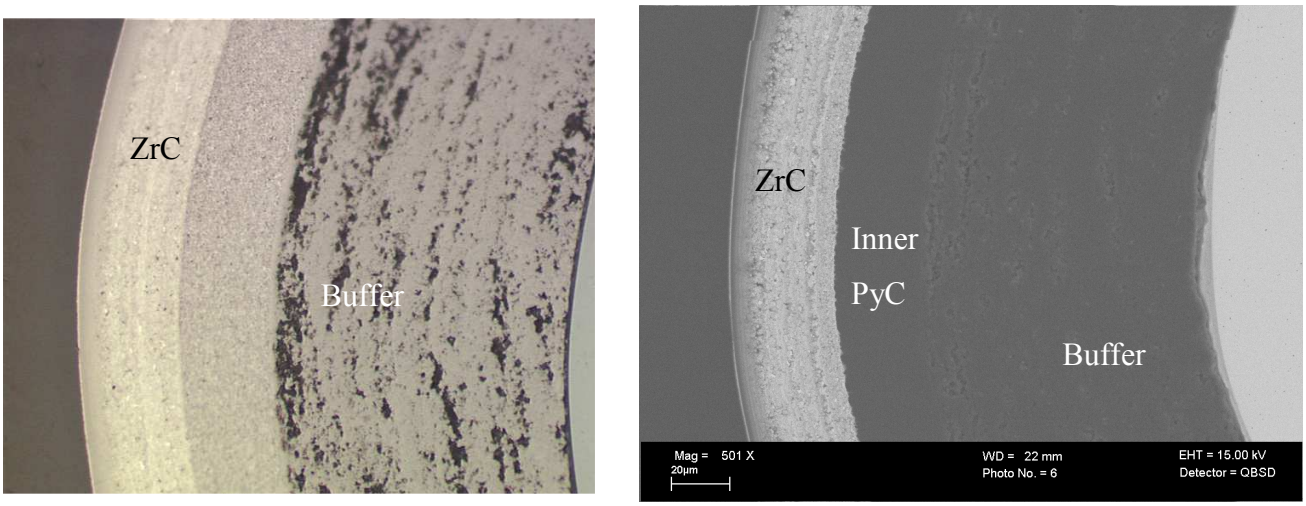

Figure IV.4: Transverse section of a particle examined under optical microscope and SEM.

5.4.4 Electron microprobe

This technique is used to make local quantitative analyses on polished sections in the form of concentration profiles across the thickness. However, in the present case, only qualitative analysis was able to be carried out on a microsphere generator, due to a missing ZrC calibration setting and spectral interferences which required an optimum analytical configuration to be found. Nevertheless, the qualitative profiles associated with the back-scattered electron image from the outer layer provide useful information (see Figure IV.5). This outer layer is composed of:

- one light-coloured layer, less than 1 µm thick, rich in zirconium, oxygen and with a minority of carbon,

- a grey layer, 2-3 µm thick, very rich in carbon and less rich in zirconium, with a constant oxygen rate throughout the layer (oxidation of ZrC surface),

- a light grey layer, 3 µm thick, showing a reduction in carbon level and an increase in zirconium,

- a light grey layer, 30 µm thick, with a heterogeneous, granular texture, characteristic of the main layer containing zirconium, carbon and chlorine in constant quantities (see Figure IV.6).

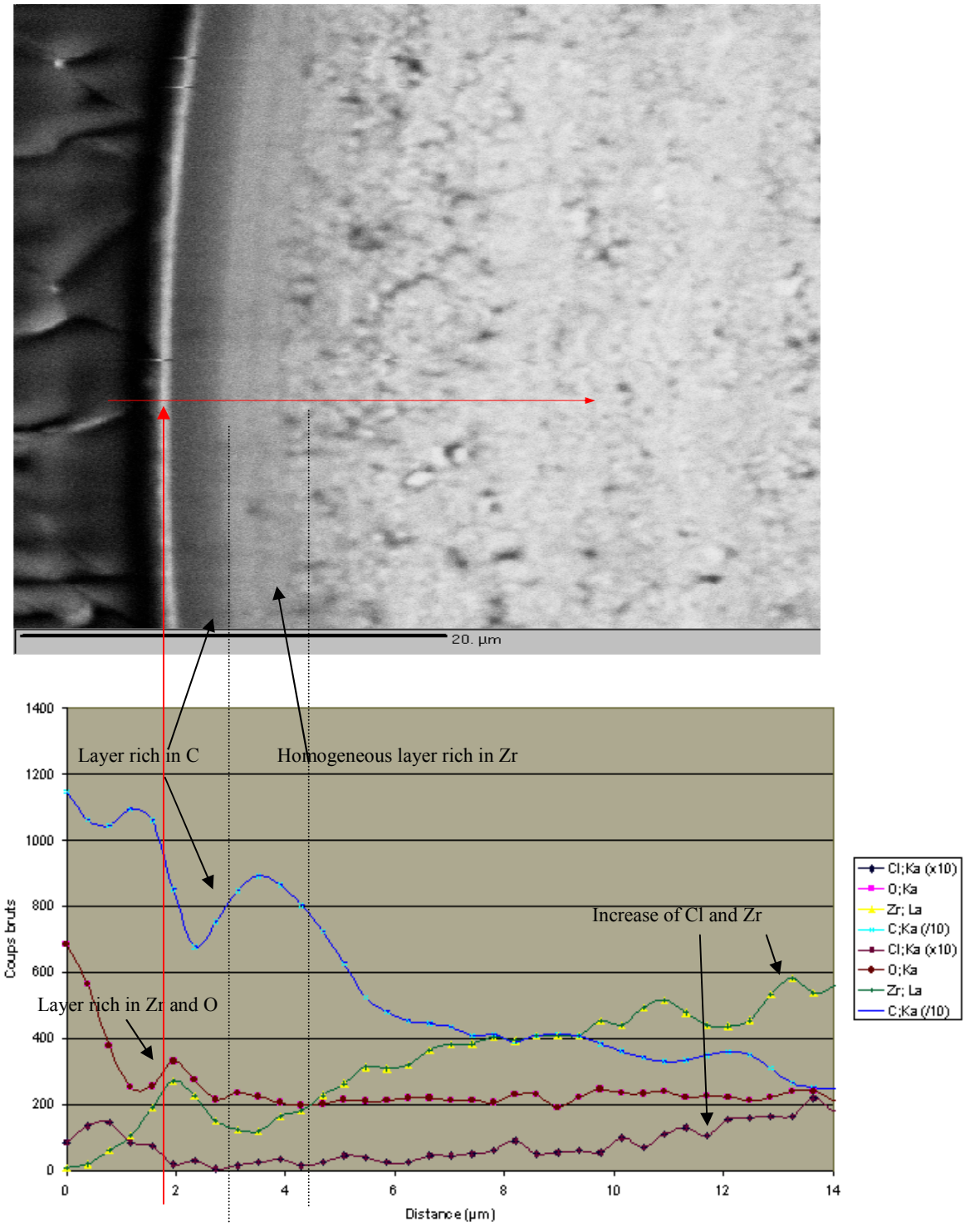

Figure IV.5: Electron probe profile of ZrC layer close to surface.

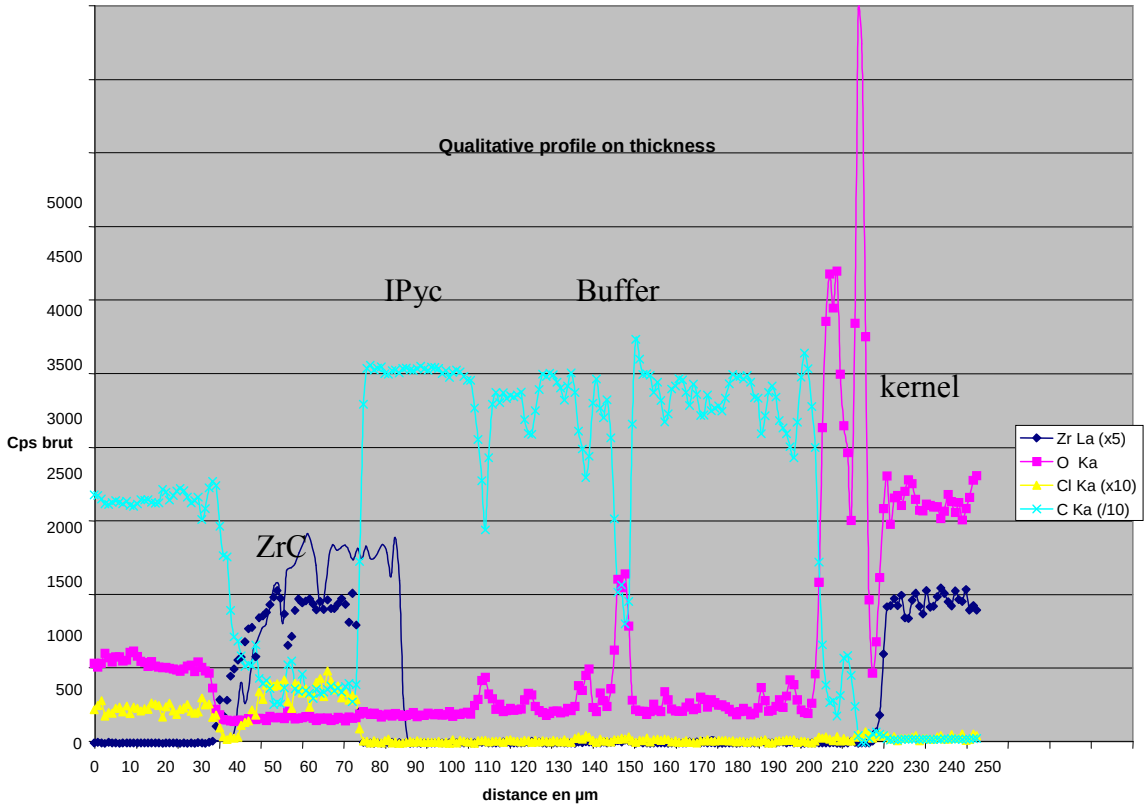

Figure IV.6: Electron probe profile of CVD layers.

5.4.5 Chemical analysis

Surface analyses by XPS-ESCA carried out at the CECAMA-ICMCB (material characterisation centre at Bordeaux institute of condensed matter chemistry) give the following composition at the microsphere surface:

- C (73 %), O (16 %), Zr (7.3 %), Cl (3.8 %) and traces of Si.

After an hour of pickling, the following results were obtained:

- Mainly Zr in form of ZrO_2 or ZrO (see microprobe analysis and back-scattered electron image),
- C in the form of free carbon.

The results of chemical analyses carried out on the particles at SCA-CNRS (central analysis department- French national scientific research centre) show a chlorine level of 0.20 % (at).

5.4.6 Summary: analysis of ZrC layer

The set of results obtained give a proper description of the ZrC layer:

- the first few outer nanometres of the layer are mainly made up of free carbon, oxygen, zirconium and chlorine (not detected by XRD), from various contaminant sources (furnace, packaging, etc…),
- a light-coloured layer, less than 1 µm thick, rich in zirconium, oxygen and with a minority of carbon in the ZrO/ZrO_2 phase (XPS-ESCA/XRD) [26],
- a grey layer, 2-3 µm thick, very rich in carbon and less rich in zirconium, with a constant oxygen rate throughout the layer (oxidation of ZrC surface), which may be constituted of C or ZrC,
- a light grey layer, 3 µm thick, showing a reduction in carbon level and an increase in ZrC, with a very low level of chlorine,
- a light grey layer, 30 µm thick, with a heterogeneous, granular texture, characteristic of the main layer made up of near- stoichometric ZrC (identified by XRD) with a maximum level of 0.2 % at of chlorine.

5.5 Limitations of the apparatus and possible improvements

The most effective conditions for obtaining a range of stoichometric ZrC is represented by a green square on the deposition graph (see figure IV.7).

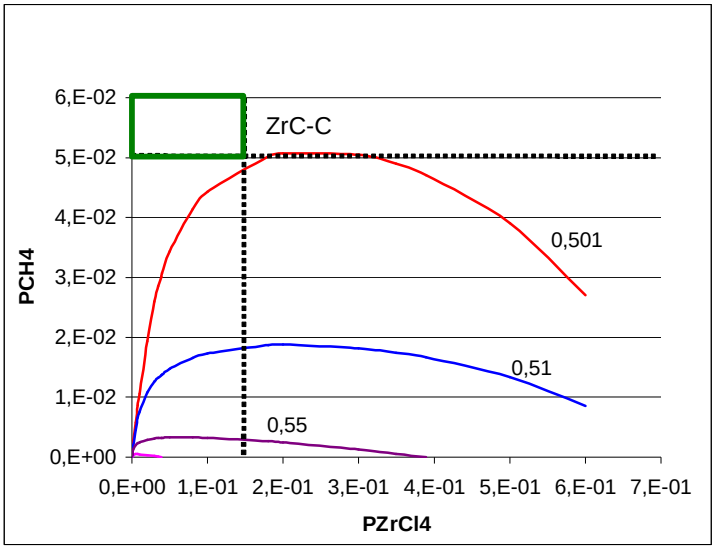

Figure IV.7: ZrC deposition graph using CH_4 at T=1,600°C and P=1atm.

The margin for adjustment is thus rather narrow: to increase this range to obtain the ideal conditions, either the $ZrCl_4$ partial pressure needs to be increased or the CH4 or C_3H_6 partial pressure needs to be reduced.

Moreover:

- to increase P_{ZrCl4}, either the argon partial pressure, which is already high, or else the total flowrate, which is limited, must be raised,
- to reduce $P_{CH4\ or\ C3H6}$, a flow rate 10 times lower must be used.
- the chlorination reaction $4HCl+Zr \rightarrow ZrCl_4+2H_2$ is highly exothermic. Indeed, the energy output, given the standard enthalpy of HCl (-92.3 kJ/mol) and $ZrCl_4$ (-869.98 kJ/mol) is 370 W per L/mn. This leads us to temperatures greater than 600 °C, limit values for the mechanical resistance of the kiln material used (stainless steel).

The temperature could be limited by limiting HCl input (see Table IV.2) into the chlorinator. However, this solution has two major disadvantages:

- significant increase in deposition time,
- reduction in propylene flowrate.

Ar flowrate (l/min)	HCl flowrate (l/min)	T top (°C)	T centre (°C)	T bottom (°C)	P Chlor. (mbar)
6.8	2.4	410	441	378	85
10	1.5	362	339	335	60
6.8	1.5	358	538	332	49
6.8	2	359	537	331	58
6.8	2.4	363	547	330	330

Table IV.2: Chlorinator temperature and pressure values according to HCl flowrate.

The propylene flowrate is set by the rotameter lower limit, i.e. 1.5 l/min. Questions could therefore be raised regarding the accuracy of the flowrate given and, in this case, it is difficult to accurately check the quantity of gas injected into the reactor, and thus whether a stoichometric deposition is made.

Technical solutions would consist of:

- putting a mass flowmeter in place which can regulate a hydrocarbon flow of the order of 0.1 $l.min^{-1}$,
- finding a kiln material for chlorination that could support the temperatures created by the reaction ,
- limiting $ZrCl_4$ as far as possible in the lines whose temperature is difficult to maintain, and to this end, limiting use of the vent to temperature increases and decreases with argon rinsing,

A feasibility study is currently underway into whether chlorination can be carried out in a graphite reactor with a lower volume (~ 2 liters) located just before the deposition furnace input. In this way, all temperature and chlorine transport issues should be dealt with.

CONCLUSION

In this study, various processes were compared for synthesising precursors that could be used for depositing zirconium carbide as a substitute for silicon carbide. Chlorination was the method selected for bringing zirconium to the reaction. This method consists of reacting zirconium in hydrogen chloride in a special reactor used for the purposes of this study.

For ZrC deposition of a well-defined composition, the precursors selected are zirconium chloride ($ZrCl_4$) for the zirconium and methane (CH_4) or propylene (C_3H_6) for carbon. The decomposition of these gases at high temperature in the fluidisation furnace, gives rise to ZrC deposition.

Our trials gave results highlighting the significance of the chlorination temperature, and particularly the importance of monitoring this temperature to avoid any chloride recondensation. A new injection pipe had to be developed. By insulating this pipe, the selected precursors could be injected during a sufficient period of time to obtain a relatively thick deposit, of 35 μm, without a blockage being formed. X-ray diffraction analysis of the material showed a mainly cubic phase (β) with ZrO_2 also present. The main layer is made up of near-stoichometric ZrC with a heterogeneous and granular texture. Poor management of chlorine and hydrocarbon distribution can explain the presence of areas that are richer or poorer in C or Zr, but having said that, development conditions selected give encouraging results. They could be optimised once technical issues associated with the limitations of the apparatus have been solved.

It will then be easier to explore the operating range, taking the thermodynamic data into consideration, and find the ideal temperature and flowrate parameters to obtain a stoichometric deposition of ZrC.

BIBLIOGRAPHY

[1] Massalki T.: **Binary alloy phase diagrams** (Ed. American society for metals, Oct. 1983)

[2] Wagner P., Hollabaugh C., Bard R.: **ZrC, a key ingredient for high-temperature nuclear fuels** (IAEA-SM-200/18, p277-287)

[3] Minato K., Ogawa T., Sawa K.: **Irradiation experiment on ZrC-coated fuel particles for high-temperature gas-cooled reactors** (Nuclear Technology, Dec. 1999, Vol.130. p272-281)

[4] Ogawa T., Fukuda K.: **Performance of ZrC coated particle fuel in irradiation and post irradiation heating tests** (J. of the American Ceramic Society, June 1992,Vol. 75,p2985-90)

[5] Pierson H**.: Handbook of chemical vapor deposition** (Noyes publication, Park Ridge, 1999, chap. the CVD of ceramic materials: carbides)

[6] Ogawa T., Ikawa K.: **Reactions of Pd with SiC and ZrC** (High Temperature Science, Dec. 1986, Vol.22, p179-193)

[7] Wagner P.: **High-temperature fuel technology for nuclear process heat: ZrC-containing coated particle fuels and high density graphite fuel matrices** (LA-6984 report, Dec. 1977)

[8] Chin J., Gantzel P.K., Hudson R.G.: **The Structure of Chemical Vapor Deposited Silicon Carbide** (GA-A13845, 15 mars 1976)

[9] Minato K., Ogawa T., Fukuda K.: **Fission product release from ZrC coated fuel particles during post-irradiation heating at 1600 °C** (J. of Nuclear Materials, Feb. 1995,Vol.224, p85-92)

[10] Minato K., Ogawa T., Fukuda K.: **Fission product release from ZrC-coated fuel particles during post- irradiation heating at 1800 °C and 2000 °C** (J. of Nuclear Materials, June 1997, Vol.249, p142-149)

[11] Etherington H.: **Nuclear engineering Handbook** (Ed. Macgraw-Hill)

[12] Hughes H., Harvey J.: **Neutron cross-sections** (Ed. Macgraw-Hill, 1955)

[13] Reynolds G.H, Kaae J.L, **Chemical vapor deposition of isotropic carbon-zirconium carbide fuel particle coatings** (General Atomics, 1975)

[14] Ogawa T., Ikawa K., Iwamoto K.: **Chemical vapor deposition of ZrC within a spouted bed by bromide process** (J. of Nuclear Materials, 1981, Vol. 97, p104-112)

[15] Ikawa K., Iwamoto K.: **Coating microspheres with zirconium carbide-carbon alloy by iodide process** (J. of Nuclear Science and Technology, June 1974, Vol.11, p263-267)

[16] Reynolds G.: **Chemical vapor deposition of ZrC on pyrocarbon-coated fuel particles** (J. of Nuclear Materials, déc.1974, Vol.50. p215-216)

[17] Hollabaugh C., Reiswig R., Wagner P., Wahman L., White R**.: A new method for coating microspheres with zirconium carbide and zirconium carbide-carbon graded coats** (LA-6012 report, Sept. 1975)

[18] Ikawa K, **Codeposition of zirconium with carbon by the bromide process** (Journal of Les-Common Metals 44, 1976)

[19] Ogawa T, Ikawa K, Iwamoto K, **Effect of gas composition on the deposition of ZrC-C mixtures** (the bromide process)

[20] Hollabaugh C., Reiswig R., Wagner P., Wahman L., White R.: **Chemical vapor deposition of ZrC made by reactions of $ZrCl_4$ with CH_4 and with C_3H_6** (Nuclear Technology, Sept. 1977, Vol.35, p527-535)

[21] Ikawa K., Iwamoto K.: **Coating microspheres with zirconium carbide-carbon alloy** (J. of Nuclear Materials, May 1974, Vol. 52 p128-130)

[22] Hollabaugh C., Reiswig R., Wagner P., Wahman L., White R.: **Factor influencing the chemical vapor deposition of ZrC** (J. of Nuclear Materials, mars 1976, Vol.62 p221-228)

[23] Van der Vis M., Cordfunke E., Konings R.: **Thermochemical properties of zirconium halides: a review** (Thermochimica Acta, May 1997, Vol. 302, p93-108)

[24] Salles P.: **Thermodynamic and experimental study into chemical vapour deposition of zirconium carbide)** (Thesis submitted in June 1986)

[25] Minato K., Ogawa T., Fukuda K.: **Review of experimental studies of zirconium carbide coated fuel particles for high temperature gas-cooled reactors** (JAERI-review 95-004, mars 1995)

[26] Cocke D.L, Owens M.S, **XPS evidence for facile formation of surface zirconium carbides from zirconium oxide overlayer decomposition and surface carbon** (Applied Surface Science 31, 1998)